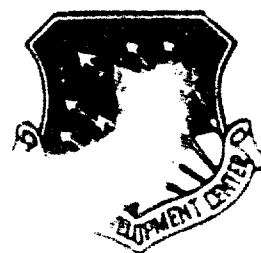


DTIC FILE COPY

2

RADC-TR-90-27  
Final Technical Report  
April 1990

AD-A222 801



# THE VARIABLY TRIMMED MEAN CFAR DETECTOR FOR NONHOMOGENEOUS BACKGROUND

University of Pennsylvania

Inci Ozgunes Tonguz and Saleem Kassam



APPROVED FOR PUBLIC RELEASE; DISTRIBUTION UNLIMITED.

Rome Air Development Center  
Air Force Systems Command  
Griffiss Air Force Base, NY 13441-5700

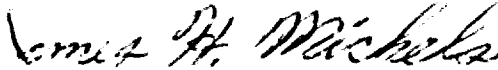
BEST  
AVAILABLE COPY

90 06 18 136

This report has been reviewed by the RADC Public Affairs Division (PA) and is releasable to the National Technical Information Service (NTIS). At NTIS it will be releasable to the general public, including foreign nations.

RADC-TR-90-27 has been reviewed and is approved for publication.

APPROVED:



JAMES H. MICHELS  
Project Engineer

APPROVED:



FRANK J. REHM  
Technical Director  
Directorate of Surveillance

FOR THE COMMANDER:



JOHN A. RITZ  
Directorate of Plans & Programs

If your address has changed or if you wish to be removed from the RADC mailing list, or if the addressee is no longer employed by your organization, please notify RADC (OCTM ) Griffiss AFB NY 13441-5700. This will assist us in maintaining a current mailing list.

Do not return copies of this report unless contractual obligations or notices on a specific document require that it be returned.

# REPORT DOCUMENTATION PAGE

Form Approved  
OPM No. 0704-0188

Public reporting burden for this collection of information is estimated to average 1 hour per response, including the time for reviewing instructions, searching existing data sources, gathering and maintaining the data needed, and reviewing the collection of information. Send comments regarding this burden estimate or any other aspect of this collection of information, including suggestions for reducing the burden, to Washington Headquarters Service, Directorate for Information Operations and Reports, 1215 Jefferson Davis Highway, Suite 1204, Arlington, VA 22202-4302, and to the Office of Information and Regulatory Affairs, Office of Management and Budget, Washington, DC 20503.

1. AGENCY USE ONLY (Leave Blank)		2. REPORT DATE April 1990	3. REPORT TYPE AND DATES COVERED Final Jul 88 - May 89	
4. TITLE AND SUBTITLE THE VARIABLY TRIMMED MEAN CFAR DETECTOR FOR NONHOMOGENEOUS BACKGROUND			5. FUNDING NUMBERS C - F30602-88-D-0027 PE - 62702F PR - 4506 TA - 17 WU - P6	
6. AUTHOR(S) Inci Ozgunes Tonguz and Saleem Kassam			8. PERFORMING ORGANIZATION REPORT NUMBER N/A	
7. PERFORMING ORGANIZATION NAME(S) AND ADDRESS(ES) University of Pennsylvania Dept of Electrical Engineering Philadelphia PA 19104			10. SPONSORING/MONITORING AGENCY REPORT NUMBER RADC-TR-90-27	
9. SPONSORING/MONITORING AGENCY NAME(S) AND ADDRESS(ES) Rome Air Development Center (OCTM) Griffiss AFB NY 13441-5700			11. SUPPLEMENTARY NOTES RADC Project Engineer: James H. Michels/OCTM/(315) 330-4431	
12a. DISTRIBUTION/AVAILABILITY STATEMENT Approved for public release; distribution unlimited.			12b. DISTRIBUTION CODE	
13. ABSTRACT (Maximum 200 words) This thesis investigates the performance of various constant false alarm rate (CFAR) detectors in both stationary noise conditions and nonideal conditions caused by multiple targets and nonuniform clutter. In particular, we introduce a new scheme for CFAR detection and called the Variably Trimmed Mean (VTM) CFAR detector. We show that this detector is a CFAR detector in exponentially distributed as well as in more general clutter distributions. A closed form analytical expression for the false alarm probability in exponentially distributed homogeneous clutter is given. We also show that in the exponentially distributed clutter situation, this detector can be designed to yield performance characteristics that are better than those of the Order Statistic and Trimmed Mean CFAR detectors.				
14. SUBJECT TERMS Adaptive CFAR Modified Trimmed Mean Detection			15. NUMBER OF PAGES 76	
			16. PRICE CODE	
17. SECURITY CLASSIFICATION OF REPORT UNCLASSIFIED	18. SECURITY CLASSIFICATION OF THIS PAGE UNCLASSIFIED	19. SECURITY CLASSIFICATION OF ABSTRACT UNCLASSIFIED	20. LIMITATION OF ABSTRACT UL	

UNIVERSITY OF PENNSYLVANIA  
THE MOORE SCHOOL OF ELECTRICAL ENGINEERING  
SCHOOL OF ENGINEERING AND APPLIED SCIENCE

THE VARIABLY TRIMMED MEAN CFAR DETECTOR  
FOR NONHOMOGENEOUS BACKGROUND

İNCİ ÖZGÜNEŞ TONGUZ

Philadelphia, Pennsylvania

August, 1989

A thesis presented to the Faculty of Engineering and Applied Science of the University of Pennsylvania in partial fulfillment of the requirements for the degree of Master of Science in Engineering for graduate work in Electrical Engineering.

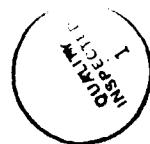
  
Thesis Supervisor : Professor Saleem A. Kassam

  
Graduate Group Chairman : Professor Sohrab Rabii

## Acknowledgement

I like to sincerely thank my advisor for his support and assistance throughout this work. Special thanks are also due to P. P. Gandhi for his help and guidance during the most difficult times. I also would like to thank Ralph Hocter, Vijitha Weracody and Chai Kim for their help in using the computing facility at Penn.

The research conducted for this thesis was supported by the Rome Air Development Center under Contract WM-55982-4-19 and by the Air Force Office of Scientific Research under Grant AFOSR 87-0052.



Accession For	
NTIS GRA&I	<input checked="checked" type="checkbox"/>
DTIC TAB	<input type="checkbox"/>
Unannounced	<input type="checkbox"/>
Justification	
By _____	
Distribution/	
Availability Codes	
Dist	Avail and/or Special
A-1	

## Dedication

This document is dedicated to my husband for his understanding and help throughout my education.

## Table of Contents

<b>List of Tables</b> . . . . .	vii
<b>List of Figures</b> . . . . .	ix
<b>1. INTRODUCTION</b> . . . . .	1
<b>2. BASIC ASSUMPTIONS AND MODEL DESCRIPTION</b> . . . . .	5
<b>3. AN OVERVIEW OF BASIC CFAR PROCESSORS</b> . . . . .	9
3.1. The CA-CFAR Processor . . . . .	9
3.2. The GO-CFAR Processor . . . . .	11
3.3. The Order Statistics CFAR Processor . . . . .	12
3.4. The TM-CFAR Processor . . . . .	14
<b>4. The VARIABLY TRIMMED MEAN CFAR DETECTOR</b> . . . . .	17
4.1. Definition of The VTM Detector . . . . .	17
4.2. Analysis of The VTM Detector . . . . .	20
<b>5. DISCUSSION Of RESULTS</b> . . . . .	30
5.1. Areas For Further Research . . . . .	32
<b>6. CONCLUSIONS</b> . . . . .	33

<b>Appendix A. Proof of Proposition 1 . . . . .</b>	<b>35</b>
<b>Appendix B. Derivation of <math>P_{fa}</math> for VTM-CFAR Processor . . . . .</b>	<b>36</b>
<b>References . . . . .</b>	<b>40</b>



## List of Tables

1. Constant scale factor T and Average Detection Threshold of GO-CFAR	
Detector. . . . .	43
2. Constant scale factor T and Average Detection Threshold of SO-CFAR	
Detector. . . . .	43
3. Constant scale factor T and Average Detection Threshold of the VTM-	
CFAR Detector with $\eta(K_2) = 1/(K_2 - k + 1)$ . . . . .	44
4. Detection performance of the adaptive- $q$ VTM detector with $q = X_{(k)}$ ,	
$N = 24$ , design $P_{fa} = 10^{-3}$ , four interfering targets, $\eta(K_2) =$	
$1/(K_2 - k + 1)$ and $SNR = 15dB$ . Note that $P_d = 0.258$ for	
the CA detector and 0.410 for the OS-CFAR detector with $k = 21$	
and 0.218 for the GO-CFAR detector. . . . .	45
5. Detection performance of the adaptive- $q$ VTM detector with $q = X_{(k)}$ ,	
$N = 24$ , design $P_{fa} = 10^{-3}$ , three interfering targets, $\eta(K_2) =$	
$1/(K_2 - k + 1)$ and $SNR = 15dB$ . Note that $P_d = 0.341$ for	
the CA detector and 0.643 for the OS-CFAR detector with $k = 21$	
and 0.282 for the GO-CFAR detector. . . . .	45

6.  $P_{fa}$  of VTM-CFAR detector with  $q = X_{(k)}$ ,  $N = 24$ , design  $P_{fa} = 10^{-3}$ ,  $\eta(k_2) = 1/(K_2 - k + 1)$  and  $CNR = 10dB$  with number of clutter cells in the window = 12. Note that  $P_{fa} = 0.021$  for the CA-CFAR detector and 0.013 for the OS-CFAR detector with  $k = 21$  and 0.004 for the GO-CFAR detector. . . . . 46
7.  $P_{fa}$  of VTM-CFAR detector with  $q = X_{(k)}$ ,  $N = 24$ , design  $P_{fa} = 10^{-3}$ ,  $\eta(k_2) = 1/(K_2 - k + 1)$  and  $CNR = 15dB$  with number of clutter cells in the window = 12. Note that  $P_{fa} = 0.024$  for the CA-CFAR detector and 0.014 for the OS-CFAR detector with  $k = 21$  and 0.004 for the GO-CFAR detector. . . . . 46

## List of Figures

1. Block diagram of typical CFAR Detector. . . . .	47
2. Mean level CFAR Detectors. . . . .	48
3. Order Statistic CFAR Detector. . . . .	49
4. Trimmed Mean CFAR Detector. . . . .	50
5. Variably Trimmed Mean CFAR Detector. . . . .	51
6. The average detection threshold ADT of OS-CFAR processor and VTM- CFAR processor with selected $\gamma$ values as a function of k. . . . .	52
7. The average detection threshold ADT of OS-CFAR processor and VTM- CFAR processor with selected $\gamma$ values as a function of k. . . . .	53
8. The average detection threshold ADT of OS-CFAR processor and VTM- CFAR processor with selected $\gamma$ values as a function of k. . . . .	54
9. Detection Performance of OS and VTM-CFAR precessors in homoge- neous background for selected parameters. . . . .	55
10. Detection Performance of CA- OS- and VTM-CFAR precessors in pres- ence of four interfering targets with selected parameters. . . . .	56
11. False alarm rate performance of GO-, OS and VTM-CFAR Detectors in clutter power transition with selected parameters. . . . .	57

12.False alarm rate performance of GO-, OS and VTM-CFAR Detectors in clutter power transition with selected parameters. . . . .	58
13.False alarm rate performance of GO-, OS and VTM-CFAR Detectors in clutter power transition with selected parameters. . . . .	59

## Chapter 1

### INTRODUCTION

The signal returns from radar targets are usually buried in thermal noise and clutter. Clutter refers to any undesired signal echo that is reflected back to the receiver by buildings, clouds, sea, etc.. Since the clutter plus noise power is unknown at any given location, a fixed threshold detection scheme cannot be applied to the radar returns in individual range cells if the false alarm rate is to be controlled. Thus, the signal processor must either be insensitive to the statistical properties of the clutter and interference or be able to adapt to a changing environment.

In this work we concentrate on the adaptive threshold CFAR processor which sets the threshold adaptively based on local information of total noise power, with noise assumed to be Gaussian distributed. The adaptive threshold CFAR processors can be divided into two classes: (1) Those that estimate clutter power based on arithmetic averaging and (2) those that regard the problem of target detection and clutter suppression more generally as a problem of signal estimation and restoration.

The most popular schemes that fall in class (1) are CA-CFAR, GO-CFAR and SO-CFAR processors. Most CFAR schemes that fall in class (2) are based on ordered observations and may be thought as versions of the L-filter, which has been used in

restoration of non-stationary signals embedded in additive noise with impulsive components [6, 7]. Here the requirements are to preserve abrupt signal transitions or edges and reduce the effects due to impulsive noise components. These requirements are related to those in radar where clutter power transition need to be suppressed and impulse-like targets detected. Trunk's OS-CFAR scheme [9] was the first that falls in class (2). Following that are the OS-CFAR, the Adaptive OS-CFAR, and the VTM-CFAR processors, the scheme that we discuss in this work.

The threshold in a CFAR detector is set adaptively by processing a group of range samples within a reference window surrounding the cell under investigation. Essentially, the threshold may be formed by determining an estimate of the local noise power in the reference window. The CFAR detector declares the presence or absence of a target in each range cell depending on whether or not the radar return exceeds the threshold. What makes one CFAR scheme different from another is the way in which the threshold is estimated. The general CFAR detection scheme is shown in Figure 1. The specifics of each CFAR processor are shown in Figures 1,2,3,4 and 5.

The CA-CFAR processor is the optimum CFAR processor when the background noise is homogeneous, that is while maintaining the constant design false alarm rate it maximizes detection probability in exponential noise and clutter. Therefore, this is the most desirable processor if there are no clutter edges and interfering targets in the reference window. However, we know that this is not a practical assumption. The CA-CFAR processor's performance significantly degrades in the presence of clutter and interference filling a non-homogeneous window (see [1]).

In the case of multiple targets the threshold estimation scheme is influenced by the

interfering signal power leading to unnecessary increase in overall threshold. This leads to masking of the primary target and thus severe degradation in detection probability. When a clutter edge is present in the reference window with a target return in the test cell, severe masking of targets results due to increase in threshold. However, if the test cell contains a clutter sample, the threshold is not high enough to achieve the design false alarm rate because the noise estimate also includes values from relatively clear background. A direct consequence of this is a significant increase in the false alarm rate. Both of these effects become worse as the clutter power increases.

The remaining schemes mentioned above were all introduced in an attempt to overcome the masking of the primary target and excessive false alarm rate caused by clutter edges and interfering targets when the CA-CFAR is used. Of all the schemes mentioned above, the GO-CFAR scheme has the best performance in presence of a worst case clutter edge in terms of false alarm rate, but it is incapable of resolving closely spaced targets. On the other hand, the OS-CFAR has the best detection performance in presence of multiple targets. Unlike the SO-CFAR, which performs very well in resolving two closely spaced targets only if they are located in the same half window, the OS-CFAR performs well regardless of the location of the interfering targets due to the ordering of the samples involved [1, 9]. The OS-CFAR processor resolves closely spaced targets effectively for proper choice of its parameter value. However, the OS-CFAR is unable to prevent excessive false alarm rate at clutter edges, unless the threshold estimate incorporates the ordered sample near the maximum, but in this case the processor suffers greater loss of detection performance [2]. The TM and the VTM-CFAR detectors are an attempt to combine the two classes of CFAR schemes mentioned earlier in order

to benefit from averaging when the background noise is homogeneous and in order to benefit from the good detection performance of OS-CFAR in multiple target situation. The VTM-CFAR can give minor improvement over the OS-CFAR detector and the VTM-CFAR processor unifies all the existing schemes by merely choosing appropriate values for its parameters.

The rest of this thesis is organized as follows. The basic assumption and model description that have been used to analyze the performance of the CFAR processor are discussed in Chapter 2. In Chapter 3, a review of the CA-CFAR, the GO-CFAR, the SO-CFAR, the OS-CFAR and the TM-CFAR processors is given along with a short discussion of their performance. In Chapter 4, the VTM-CFAR detector is discussed and is shown to possess the CFAR property, provided that some mild conditions are met. An analytical expression is obtained for the probability of false alarm and probability of detection as well as the ADT of the VTM-CFAR in homogeneous background. In Chapter 5, we present some simulation results and discuss the results obtained. The overall conclusions of the study are given in Chapter 6. Most of the derivations and proofs are relegated to the Appendices in order to enhance the main thrust of the study.



## Chapter 2

### BASIC ASSUMPTIONS AND MODEL DESCRIPTION

In a general CFAR detection scheme the square-law detected video range samples are sent serially into a shift register of length  $N_s + 1 = 2n + 1$  as shown in Figure 1. The statistic  $Z$  which is proportional to the estimate of total noise power is formed by appropriately processing the  $N$  reference cells surrounding the test cell containing the candidate for a target  $Y$ . Threshold is equal to  $TZ$  where  $T$  is a constant scale factor used to achieve a desired constant false alarm probability for a given window of size  $N$  when the total background noise is homogeneous. A target is declared to be present if  $Y > TZ$ ; otherwise no target is declared. The way statistic  $Z$  is obtained leads to different CFAR schemes. For example, in the CA-CFAR processor,  $Z$  is sum of the range samples; in GO-CFAR,  $Z$  is  $\max(\text{Sum1}, \text{Sum2})$  where Sum1 is sum of the leading  $N/2$  samples and Sum2 is sum of the lagging  $N/2$  samples.

In order to analyze the detection performance of a CFAR processor in homogeneous background noise, we assume that the samples  $X_1, \dots, X_N$  and  $Y$  are iid and exponentially distributed, with probability density function

$$f(x) = \begin{cases} \frac{1}{2\lambda} e^{-\frac{1}{2\lambda}x} & x \geq 0 \\ 0 & \text{otherwise.} \end{cases} \quad (2.1)$$

Under the null hypothesis  $H_0$  of no target in a range cell and homogeneous background,

$\lambda$  is the total background clutter-plus thermal noise power , which is denoted by  $\mu$ .

Under the alternative hypothesis  $H_1$  of presence of a target ,  $\lambda$  is  $\mu(1 + S)$ , where  $S$  is the average signal-to-noise ratio (SNR) of a target. This means that we are assuming a Swerling I model for the radar returns from a target and Gaussian statistics for the background. We also assume that the observations in the  $(N + 1)$  cells are statistically independent. Therefore, for the cell under test the value of  $\lambda$  in (2.1) is

$$\lambda = \begin{cases} \mu & \text{under } H_0 \\ \mu(1 + S) & \text{under } H_1 \end{cases} \quad (2.2)$$

and for the  $N$  cells surrounding the cell under test  $\lambda$  always equals  $\mu$  [2].

In our analysis and study of the non-homogeneous background for which the reference cells do not follow a single common probability density function (pdf), we are concerned with transitions or changes in power  $\lambda$  and presence of multiple targets in the window. In the case of transitions, we consider the case of a single transition from a lower total noise background power level to a higher level. Thus, we assume that a portion of the reference cells have thermal noise only with  $\lambda = \mu = \mu_0$  and the remaining reference cells arise from a clutter background with thermal noise so that  $\lambda = \mu = \mu_0(1 + C)$ , with  $C$  being the clutter-to-noise ratio (CNR). The extent of the physical clutter area is assumed to be at least as large as the size of the reference window so that the reference window does not contain multiple clutter patches [2]. In the case of multiple target environment, the amplitudes of all the targets present in the reference window are assumed to fluctuate according to the Swerling I model. The common interference-to-total noise ratio (INR) of all extraneous targets is denoted by  $I$ . Thus, for reference cells containing extraneous targets the value of  $\mu$  in equation (1)

is  $\mu(1 + I)$ . We are interested in detection performance as a function of primary target SNR for different values of interference-to-signal ratio (i.e  $I/S$ ).

It is crucial to note that the performance in homogeneous background of a CFAR processor is independent of the total power  $\mu$ , whether it be thermal noise power or clutter-plus-thermal noise power. Therefore, only changes in the total noise power caused by regions of clutter power transitions and multiple target environment influences the overall processor performance. Naturally, the most desirable CFAR processor would be one that is least sensitive to changes in the total noise power within the window of reference cells so that a constant false alarm rate is maintained.

The processor performance is determined by average detection and false alarm probabilities. Probability of false alarm,  $P_{fa}$  is determined in general by

$$P_{fa} = E \{ P \{ Y > TZ / H_0 \} \}. \quad (2.3)$$

Since  $Y \sim \frac{1}{2\mu} e^{-\frac{1}{2\mu}y}$ ,  $0 < y < \infty$

$$\begin{aligned} P_{fa} &= E \left\{ \int_{TZ}^{\infty} \frac{1}{2\mu} e^{-\frac{1}{2\mu}y} dy \right\} \\ &= E \left\{ e^{-\frac{1}{2\mu}TZ} \right\} \\ &= M_Z(T/2\mu) \end{aligned} \quad (2.4)$$

where  $M_Z(.)$  denotes the moment generating function (mgf) of the random variable  $Z$ .

Similarly, the detection probability  $P_d$  is given by

$$P_d = E \{ P \{ Y > TZ / H_1 \} \}. \quad (2.5)$$

Since under the signal-present hypothesis  $H_1$  the mean  $2\lambda = 2\mu(1+S)$ , we can determine

$P_d$  by simply replacing  $\mu$  with  $\mu(1 + S)$  in (2.4) i.e.,

$$P_d = M_Z [T/2\mu(1 + S)]. \quad (2.6)$$

Following the discussion above, it follows that, for a CFAR scheme,  $M_Z(T/2\mu)$  must be independent of  $\mu$ . *If for a scheme  $M_Z(T/2\mu)$  is not independent of  $\mu$ , then it is not a CFAR scheme.*

Since there are several different CFAR schemes, it is important to have a reliable way of comparing their performances. One way is to compare their false alarm rate performance in presence of clutter edges. A second way is to compare their detection performance and a third way is to compare the ADT (Average Detection Threshold) for each processor. The ADT is also useful because comparison of the fixed optimum threshold with ADT of a CFAR processor gives a measure of the overall loss of detection without the need to calculate the detection probability. From [2]

$$ADT = E(TZ)/2\mu. \quad (2.7)$$

For the optimum detector the the ADT is simply  $-\ln(P_{fa})$  [2]. From probability theory (see [15, 16] on moment generating functions), we know that

$$E(Z) = -2\mu \frac{d}{dT} M_Z(T/2\mu)|_{T=0} \quad (2.8)$$

Therefore,

$$ADT = -T \left\{ \frac{d}{dT} P_{fa}|_{T=0} \right\} \quad (2.9)$$

It is important to note that for any CFAR scheme the ADT is independent of  $\mu$  because  $P_{fa}$  is independent of  $\mu$ . The rest of this work will be based on these assumptions unless otherwise stated.

## Chapter 3

### AN OVERVIEW OF BASIC CFAR PROCESSORS

The CFAR processors that will be discussed in this chapter are well known and they have been included in this thesis for ease of comparison with the VTM-CFAR that we study. A thorough discussion of these schemes can be found in [2].

#### 3.1 The CA-CFAR Processor

For the CA-CFAR processor

$$Z = \sum_{i=1}^N X_i. \quad (3.1)$$

Using the result given in (2.4)

$$\begin{aligned} P_{fa} &= M_Z(T/2\mu) \\ &= E \left\{ e^{-\frac{T}{2\mu} T Z} \right\} \\ &= E \left\{ e^{-\frac{T}{2\mu} \sum_{i=1}^N X_i} \right\}. \end{aligned} \quad (3.2)$$

Using the well known result that for the iid random variables  $X_1, \dots, X_N$

$$E \{ g(X_1) g(X_2) \dots g(X_n) \} = E[g(X_1)] \dots E[g(X_1)]$$

$$\begin{aligned} P_{fa} &= \prod_{i=1}^N E \left\{ e^{-\frac{T}{2\mu} X_i} \right\} \\ &= \frac{1}{(1 + T)^N}. \end{aligned} \quad (3.3)$$

It follows from expression (3.3) that

$$P_d = \left[ 1 + \frac{T}{(1+S)} \right]^{-N}. \quad (3.4)$$

We can also compute the constant scale factor from (3.3) to be

$$T = P_{fa}^{-1/N} - 1. \quad (3.5)$$

For the CA-CFAR detector substitution of expression (3.3) into expression (2.9) yields

$$ADT = NT. \quad (3.6)$$

In non-homogeneous background, assuming that the reference window contains  $r$  cells from clutter background with noise power  $\mu_0(1+C)$  and  $(N-r)$  cells from clear background with noise power  $\mu_0$ , then

$$Z = \sum_{i=1}^r X_i + \sum_{i=r+1}^N X_i. \quad (3.7)$$

There are two interesting situations to consider under these circumstances. One is when the cell under investigation comes from a clear background. This yields,

$$P_{fa} = [1 + (1+C)^T]^{-r} [1+T]^{r-N}. \quad (3.8)$$

The other is when the cell under investigation comes from a clutter background. This yields,

$$\begin{aligned} P_{fa} &= M_Z \left( \frac{T}{2\mu_0(1+C)} \right) \\ &= (1+T)^{-r} (1+T/(1+C))^{r-N} \end{aligned} \quad (3.9)$$

In the case of multiple targets,

$$P_d = [1 + (1+I)T/(1+S)]^{-r} [1+T/(1+S)]^{r-N} \quad (3.10)$$

where  $r$  represents the number of interfering targets present in the reference window.

The performance of the CA-CFAR processor is compared with those of other CFAR processors as we study the others.

### 3.2 The GO-CFAR Processor

For the GO-CFAR processor

$$Z = \max(\text{Sum1}, \text{Sum2}) \quad (3.11)$$

where  $\text{Sum1} = \sum_{i=1}^{N/2} X_i$  and  $\text{Sum2} = \sum_{i=N/2+1}^N X_i$ . When the background noise is homogeneous, the false alarm probability is found by using expression (2.4), which requires the computation of the mgf of  $Z$  which is easily computed, and we obtain:

$$P_{fa} = 2(1+T)^{-n} - 2 \sum_{i=0}^{n-1} \binom{n+i-1}{i} (2+T)^{-(n+i)}. \quad (3.12)$$

As explained before, the detection probability  $P_d$  is found by simply replacing  $T$  with  $T/(1+S)$  in (3.12).

The ADT for the GO-CFAR processor is found by using equation (2.9)

$$\text{ADT} = 2T \left[ n - \sum_{i=0}^{n-1} \binom{n+i-1}{i} (i+n) 2^{-(n+i+1)} \right]. \quad (3.13)$$

Table 1 lists the values of  $T$  and the ADT for various design  $P_{fa}$ .

When the reference window contains a cluster edge or multiple targets, an exact  $P_{fa}$  expression can be found (see [2]). Since the purpose here is to compare the GO-CFAR detector with the VTM-CFAR detector for which an exact expression under these circumstances is not available, we obtain the  $P_{fa}$  and  $P_d$  values for the GO-CFAR detector using Monte Carlo simulations. Numerical values will be given and discussed

at the end of the thesis; therefore, for the time-being, we note that this processor has the best performance among all the CFAR processors in terms of false alarms at clutter edges. What makes this processor undesirable is the intolerable masking of the primary target which is worse than the CA-CFAR processor.

We will not discuss the Smallest Of (SO) CFAR processor here, but we mention that although it was introduced as a solution to detection loss in multiple target situation, the Order Statistics (OS) CFAR scheme that will be discussed next is superior to the SO-CFAR scheme; because, unlike the SO-CFAR scheme, the detection performance of the OS-CFAR detector is independent of the location of the interfering targets. Thus, the SO-CFAR processor is not an interesting processor and will not be compared to the VTM-CFAR detector.

### 3.3 The Order Statistics CFAR Processor

The OS-CFAR detector is designed to overcome the problem of the loss of detection performance suffered by the CA-CFAR and the GO-CFAR detectors when the interfering targets are in the background. In a processor based on just averaging, in presence of interfering targets in the reference window, the statistic  $Z$  has a larger value than the average noise power in the window and this causes a large loss of detection. To alleviate this problem in the OS detector the reference range samples  $X_1, \dots, X_N$  are first ordered in ascending order and then the statistic  $Z$  is formed as

$$Z = X_{(k)} \quad (3.14)$$



where  $X_{(i)}$  is the largest sample in the reference window,  $i = 1, \dots, N$  and  $1 \leq k \leq N$  is an integer valued design parameter. The value of  $k$  is chosen to eliminate the background cells with the largest voltages in order to optimize detection performance. Since the cells with the largest voltages are likely to be interfering targets, by using this method the influence of interfering targets are eliminated leading to a statistic  $Z$  which is more representative of the background noise power. Consequently, there is not a large loss in detection performance when interfering targets are in the background cells.

The false alarm probability and the ADT expressions for the OS-CFAR processor are derived in [2] and therefore only the final results will be presented here.

In homogeneous background,

$$P_{fa} = \prod_{i=0}^{k-1} \frac{(N-i)}{(N-i+T)} \quad (3.15)$$

and it follows that

$$P_d = \prod_{i=0}^{k-1} \frac{(N-i)}{(N-i+T/(1+S))} \quad (3.16)$$

and

$$ADT = T \sum_{i=0}^{k-1} \frac{1}{(N-i)} \quad (3.17)$$

We note that  $T$  is a function of  $k$  and as shown in [2] as  $k$  increases  $T$  decreases in order to compensate for the increase in  $Z$  and thus maintain the design false alarm rate.

It is shown in [2] that the ADT exhibits a broad minimum for larger values of  $k$ . Thus, as explained before, any reasonable  $k$  for which ADT is relatively low may be chosen for estimating the noise power without sacrificing the detection performance in uniform noise background.

As explained in [2], in stationary clutter the detection performance of the OS-CFAR

improves until  $k$  reaches 21 when  $N = 24$  where  $P_d$  achieves the maximum value and the ADT the minimum. For  $k$  greater than 21, the  $P_d$  degrades or equivalently the ADT increases. Thus, for  $N = 24$  and stationary clutter, the optimum value of  $k$  is 21 [2, 3]. Although the OS detector can discriminate the primary target from up to  $(N - k)$  interferers, it is shown in [2] that unless  $k$  is chosen to be a number close to  $N$ , i.e.,  $k = N$ , the false alarm rate of the OS-CFAR detector can increase substantially in presence of clutter power transitions. However, as shown by [2] such a value for  $k$  is not generally desirable because the corresponding OS-CFAR detector not only suffers some loss of detection performance in stationary clutter but it also fails to detect the primary target in presence of multiple targets. In conclusion, the OS-CFAR processor performance is significantly worse compared to the GO-CFAR processor in presence of clutter edges and it exhibits some loss of detection power in homogeneous noise background compared to the CA and GO-CFAR processors; however, its performance is superior in a multiple target environment.

For the interested reader we would like to add that closed form expressions for the  $P_{fa}$  and the  $P_d$  in presence of clutter edges and multiple targets can be found in reference [2]. Our values for comparison with the VTM-CFAR detector in these situations will be obtained using Monte Carlo simulation, the same way that the data for the VTM-CFAR detector will be obtained.

### 3.4 The TM-CFAR Processor

This is one of the first attempts to combine the benefits of averaging and ordering+censoring. In this scheme the noise power is estimated by a linear combination of

some selected ordered range samples. The linear combination may be anticipated to give better results because averaging estimates the noise power more efficiently as in the case of the CA-CFAR and the GO-CFAR processors and thus loss of detection in uniform background is more tolerable.

In the TM-CFAR detector the statistic  $Z$  is obtained by censoring  $T_1$  ordered range samples from below and  $T_2$  ordered range samples from above and then forming a sum of the remaining samples. Thus,

$$Z = \sum_{i=T_1+1}^{N-T_2} X_{(i)} \quad (3.18)$$

where  $T_1$  and  $T_2$  are the upper and lower trimming parameters, respectively, satisfying conditions  $0 \leq T_1, T_2 < N$  and  $T_1 + T_2 < N$ .

It helps to realize that OS- and CA-CFAR schemes are special cases of the TM-CFAR scheme. Namely, when  $T_1 = k - 1$  and  $T_2 = N - k$  the TM-CFAR scheme reduces to the OS-CFAR scheme and when  $T_1 = T_2 = 0$  the TM-CFAR scheme reduces to the CA-CFAR scheme.

The  $P_{fa}$  and the ADT in homogeneous background for this scheme are derived in [2]; here we give a slightly simpler version of the ADT. As derived in [2] (see equation (48))

$$P_{fa} = \prod_{i=1}^{N-T_1-T_2} M_{V_i}(T) \quad (3.19)$$

where

$$M_{V_i}(T) = \prod_{i=0}^{T_1} \frac{(N-i)}{[N + T(N - T_2 - T_1) - i]} \quad (3.20)$$

and

$$M_{V_i}(T) = \frac{a_i}{a_i + T} \quad i = 2, \dots, N - T_1 - T_2 \quad (3.21)$$

where

$$a_i = \frac{(N - T_1 - i + 1)}{(N - T_1 - T_2 - i + 1)}. \quad (3.22)$$

As usual, the detection probability  $P_d$  is obtained by replacing  $T$  with  $T/(1 + S)$  in (3.19). The loss of detection in terms of the ADT is computed simply by using (2.9) which yields

$$ADT = T \left\{ (N - T_2 - T_1) \sum_{i=0}^{T_1} \frac{1}{(N - i)} + \sum_{i=2}^{N-T_2-T_1} \frac{(N - T_1 - T_2 - i + 1)}{(N - T_1 - i + 1)} \right\}. \quad (3.23)$$

As shown and explained by [2], symmetric trimming is not very interesting, because it does not give a performance advantage over the other CFAR schemes in regions of clutter transitions. However, asymmetric trimming can be made more interesting with the right choice of  $T_1$  and  $T_2$  values. In fact, it has been shown in [2] that the sum of more than one ordered range samples that is incorporated in the TM detector leads to some improvement in the detection performance in exponential stationary clutter over that of the OS detector [2]. It is also shown in [2] that a relatively high value for  $T_1$  is required to reduce degradation in the false alarm rate of the TM detector at clutter edges with only minor loss of detection performance in stationary clutter. Furthermore, the TM detector can discriminate the primary target from up to  $T_2$  interferers.

Since the performance of the TM-CFAR detector is very close to the performance of the OS-CFAR detector, it is sufficient to provide numerical results for only the OS-CFAR detector..

## Chapter 4

# The VARIABLY TRIMMED MEAN CFAR DETECTOR

### 4.1 Definition of The VTM Detector

The motivation for using this procedure came from the similarity of the requirements of radar where clutter power transitions need to be suppressed and impulse like targets detected, and the restoration of nonstationary signals embedded in additive noise with impulsive components [6, 7] . The recent literature in the latter topic has shown that the Modified Trimmed Mean (MTM) filter, which is related to both the L-filters and the class of M-filters [7], has good performance at signal edges. Hence, we decided to use the idea of the modified trimmed mean (MTM) filter for CFAR radar detection to alleviate the problems at clutter edges and multiple target situation.

We called our processor Variably Trimmed Mean (VTM) because of the way the samples are trimmed, namely, data adaptively. For this detector, the statistic  $Z$  is obtained as follows.

$$Z = \eta(K_2) \sum_{i=k}^{K_2} X_{(i)} \quad (4.1)$$

where integer valued  $k$  is the index of the smallest ordered sample in the sum and is a design value between 1 and  $N$ ,  $k \leq K_2 \leq N$  is a discrete random variable whose value

is determined based on a data-dependent rule, and the  $\eta(K_2)$  is some appropriately chosen normalizing coefficient. The VTM detector can therefore be thought of as a TM detector with a fixed lower trimming  $T_1 = k - 1$  and a variable upper trimming  $T_2 = N - K_2$ . The data-dependent rule that sets the value of  $K_2$  in each processing window is defined as follows:

$$K_2 = k_2 \text{ iff } X_{(k_2)} \leq X_{(k)} + q < X_{(k_2+1)}, \quad k \leq k_2 \leq N \quad (4.2)$$

where  $q$  is a design parameter which may or may not be fixed. This procedure can be thought of as performing a separate experiment on  $X_{(i)}, i = 1, \dots, N$  to compute the value  $K_2 = k_2$  in every window. A block diagram of the VTM detector is shown in Figure 5.

The operation of the VTM detector can alternatively be explained as follows: First the values of the design parameters  $N, T, k, q$  and  $\eta(K_2)$ ,  $k \leq K_2 \leq N$ , are selected. In each processing window, an interval of size  $q$  is formed above and including  $X_{(k)}$ , and those range samples whose values fall within the interval  $[X_{(k)}, X_{(k)} + q]$  are used to determine the statistic  $Z$ . The normalizing coefficients can simply be  $1/(K_2 - k + 1)$ ,  $k \leq K_2 \leq N$ , which scales the sum of (4.1) according to the number of ordered samples used. The  $\eta(K_2)$  can also be picked to be unity. We assume that the  $\eta(K_2)$  depends only on the values of  $N, k$  and  $q$ , and is independent of the design  $P_{fa}$ . The parameter  $T$ , on the other hand, is tuned to achieve the design  $P_{fa}$ . The value of  $q$  determines, on the average, the number of range samples incorporated in the sum. Clearly, the VTM-CFAR detector reduces to the OS-CFAR detector with parameter  $k$  as  $q \rightarrow 0$  and to the TM-CFAR detector with  $T_1 = k - 1$  and  $T_2 = 0$  as  $q \rightarrow \infty$ . We will show in the next section that a VTM detector with a fixed  $q$  will not result in a CFAR detector;

however, a detector in which  $q$  is set proportional to  $X_{(i)}$  for some  $i$  in each reference window, is shown to be CFAR.

A VTM detector with a more general rule can be defined where a symmetric interval of size  $2q$  is placed around  $X_{(k)}$  and range samples whose values fall in  $[X_{(k)} - q, X_{(k)} + q]$  are used to compute  $Z$ . However, we chose not to do so for reasons that will become clear shortly.

For a given  $k$ , the value of  $q$  can be chosen to maximize the detection performance in a homogeneous reference window. This is achieved by selecting the smallest value of  $q$  that leads to a situation where almost all of the range samples larger than  $X_{(k)}$  are used to obtain  $Z$ . When the reference window contains multiple interfering targets, the corresponding range cells will generally be larger than  $X_{(k)} + q$ , for a properly chosen  $k$ . Hence, the value of  $k$  must be less than the maximum number of interferers that may appear in the reference window to guarantee satisfactory detection performance in a multiple target environment.

On the other hand, when a few range samples (less than  $N - k$ ) from a high-clutter region enter the reference window, they look like interfering targets to the VTM detector and tend to be discarded. The false alarm rate and detection performance characteristics are only slightly degraded since  $X_{(k)}$  is still chosen from samples that come from a low-clutter region. When the number of high-clutter samples exceeds  $N - k$ ,  $X_{(k)}$  is now one of the high-clutter samples. Hence, most of the samples larger than  $X_{(k)}$  will now be included in obtaining  $Z$ . This leads to a considerable increase in the threshold, which in turn helps to control the false alarm rate when the test cell  $Y$  contains a range sample from the high-clutter region. Therefore, in practice, for

exponential clutter,  $k$  should be chosen as large as possible to prevent excessive false alarms at the clutter edge. This conclusion is similar to the one reached in [2] for the TM detector where the lower trimming parameter  $T_1$  was set to a high value to reduce the degradation in the false alarm rate caused by regions of clutter power transitions.

A special case of the VTM CFAR detector, namely, the Excision CFAR detector, has recently been analyzed in a multiple target environment in which the value of  $k$  is set to unity [10]. Here  $k_2$  is chosen to satisfy the condition  $X_{(k_2)} \leq \bar{q} < X_{(k_2+1)}$  for some real-valued design parameter  $\bar{q}$ . Clearly, the false alarm rate performance of this detector will degrade considerably in regions of clutter power transitions because, the detector will almost always censor samples from a high clutter region even if the test cell is from the high clutter region itself. Hence, it is essential that the size- $q$  interval be formed around a  $k^{\text{th}}$  smallest range sample, with  $k > n$ .

## 4.2 Analysis of The VTM Detector

In this section we will show that the VTM detector is a CFAR detector provided that  $q$  is chosen properly. Let us define the event  $E_{k_2}$  by :

$$E_{k_2} : X_{(k_2)} \leq X_{(k)} + q < X_{(k_2+1)}. \quad (4.3)$$

The false alarm probability of the VTM detector, which is defined to be the probability that a noise sample in the test cell exceeds the threshold in a stationary clutter environment, is given by

$$\begin{aligned} P_{fa} &= P[Y > TZ] \\ &= \sum_{K_2=k}^N P[Y > TZ(K_2) | E_{k_2}] P[E_{k_2}] \end{aligned}$$



$$= \sum_{K_2=k}^N P[Y > TZ(K_2), E_{k_2}] \quad (4.4)$$

where  $Z(K_2) = \eta(K_2) \sum_{i=k}^{K_2} X_{(i)}$  and  $Y$  is a noise sample. Note that  $Z$  and  $Z(K_2)$  are two different statistics; the former is a function of  $X_{(1)}, \dots, X_{(N)}$  whereas the latter is a function of only  $X_{(k)}, \dots, X_{(K_2)}$ . It is worth mentioning again that the expression (4.4) for the  $P_{fa}$  must be independent of the total noise power  $\mu$  for the VTM detector to be CFAR in stationary clutter. To prove that this is in fact true, we refer to [4] where a general proof is given. We include that proof here, for completeness.

First some definitions to facilitate the proof are introduced. Let  $\mathbf{X}$  be the vector  $(X_1, \dots, X_N)$  of  $N$  real-valued random variables (in our context,  $\mathbf{X}$  can be thought of as the vector of range samples in a reference window).

**Definition 1** An event  $A(\mathbf{X})$  is called scale invariant iff  $A(\tau\mathbf{X}) = A(\mathbf{X})$  for all real-valued  $\tau > 0$ .

**Definition 2** A family  $f_{\mathbf{X}}(\mathbf{x}; \mu, \underline{\theta})$  of densities of  $\mathbf{X}$  parameterized by real-valued parameter  $\mu > 0$  and  $\underline{\theta}$  is said to have a scale parameter  $\mu$  iff  $f_{\mathbf{X}}(\mathbf{x}; \mu, \underline{\theta}) = (1/\mu^n)g(\mathbf{x}/\mu; \underline{\theta})$  where  $g(\cdot; \underline{\theta})$  is some density function independent of  $\mu$ .

**Proposition 1** Let  $f_{\mathbf{X}}(\mathbf{x}; \mu, \underline{\theta})$  be a family of densities with scale parameter  $\mu$ . Further, let  $A_1(\mathbf{X}), A_2(\mathbf{X}), \dots, A_m(\mathbf{X})$ ,  $m$  finite, be some scale invariant events. Then  $P[A_1(\mathbf{X}), A_2(\mathbf{X}), \dots, A_m(\mathbf{X})]$  is independent of  $\mu$ .

Proof of this proposition is given in Appendix A. We have the following corollary as a simple consequence of the proposition.

**Corollary 1** Let  $X_i, i = 1, \dots, N$  be iid random variables governed by a common probability density function (pdf)  $f_X(x; \mu, \underline{\theta})$ , and  $Y$  be a random variable independent of  $X_i, i = 1, \dots, N$  with pdf  $f_Y(y; \mu, \bar{\theta})$  where  $\mu$  is the common scale parameter. Then  $P[Y > TZ(k_2), E_{k_2}]$  is independent of  $\mu$  if  $q/\mu$  is a fixed constant, or if  $q$  is a linear function of  $X_{(i)}, i = 1, \dots, N$ .

The event  $Y > TZ(K_2)$  is clearly scale invariant, whereas  $E_{K_2}$  is scale invariant provided that the condition described in the corollary is satisfied. The proof of the corollary then follows from the fact that the joint pdf of  $X_{(k)}, \dots, X_{(K_2+1)}$  also has  $\mu$  as a scale parameter.

With the aid of the above proposition, all of the CFAR schemes considered previously which assume exponentially distributed stationary clutter and target model can be shown to be CFAR, without actually computing the expression for the false alarm rate. More generally, these schemes will remain CFAR even if the distributions of the noise and target returns do not obey the commonly assumed exponential distribution, but are governed by arbitrary distributions with a common scale parameter proportional to the total noise power and other parameters independent of noise power. This fact can be used in further study when the samples are assumed to have a Rayleigh instead of an exponential distribution. Since Rayleigh distribution has a lighter tail than exponential distribution the variable trimming along with the averaging operation incorporated in the VTM detector may give better results than exponential distribution assumption.

In the case of VTM detector we have the following two cases:

*Fixed- $q$  VTM Detector:* Clearly if  $q$  is fixed, then the VTM detector is not CFAR. A

different approach can be taken in which the ideas of conditional-tests may be employed to the fixed- $q$  VTM detector. Here, the multiplier  $T$  which is a function of  $N$ , the design  $P_{fa}$ ,  $k$  and  $q$  is allowed to vary with  $K_2$ .  $K_2$  is computed by satisfying the condition  $P[Y > T(K_2)Z(K_2) | E_{K_2}] = P_{fa}$ . The overall  $P_{fa}$  in this case no longer depends on the  $P(E_{K_2})$  (see equation (4.4)). Such a VTM detector is still not a CFAR detector since  $T(K_2)$  depends on the value of  $\mu$ . However, our simulation results indicate that the influence of  $q$  on  $T(K_2)$  is relatively weak and that the false alarm rate remains nearly constant for a noise power variation of 30 dB.

*Adaptive- $q$  VTM Detector:* Here, the value of  $q$  is adaptively set in each window from the reference range samples. In particular, we propose to set  $q$  such that

$$q = \gamma X_{(k)} \quad (4.5)$$

where  $\gamma \geq 0$  is a preselected design parameter. As a matter of fact, any other order statistic  $X_{(i)}$  can be used in place of  $X_{(k)}$  in equation (4.5). The constant multiplier  $T$  now depends on  $k$  and  $\gamma$  for fixed  $N$  and the design  $P_{fa}$ . The event  $E_{k_2}$  of equation (4.3) becomes

$$E_{k_2} : X_{(k_2)} \leq X_{(k)} + \gamma X_{(k)} < X_{(k_2+1)} \quad (4.6)$$

or

$$E_{k_2} : X_{(K_2)} - (1 + \gamma)X_{(k)} \leq 0 < X_{(K_2+1)} - (1 + \gamma)X_{(k)} \quad (4.7)$$

and is now scale invariant. Hence, the adaptive- $q$  VTM detector is a true CFAR detector.

The basic steps in deriving the closed-form expression for the  $P_{fa}$  of the adaptive- $q$  VTM detector along with the final closed form expression is presented below. In order

to make the thesis more readable, the detailed derivation is given in Appendix B.

We start the derivation of the false alarm probability by using the result from chapter 2, namely

$$P_{fa} = E\{e^{-\frac{1}{T\mu}TZ}\} \quad (4.8)$$

Since it has been established that for the adaptive- $q$  VTM detector this is independent of  $\mu$ , for simplicity we will set  $\mu = 1/2$ . We will also assume that  $\eta(K_2) = 1$ . Therefore, equation (4.8) reduces to

$$\begin{aligned} P_{fa} &= E\{e^{-TZ}\} \\ &= E\left\{e^{-T\sum_{j=k}^{K_2} X_{(j)}}\right\} \\ &= b_k \end{aligned} \quad (4.9)$$

where, as established before  $k$  is a fixed deterministic integer valued variable which can have a value between 1 and  $N$ . In order to make the derivation more comprehensive, we can think of  $K_2$  as the last time that  $X_{(j)} \leq (1 + \gamma)X_{(k)}$ . We also introduce the notation  $b_k$  in order to keep track of the derivation which, as will be obvious soon, has a backward iteration nature.

Using the indicator function to facilitate our derivation, we proceed as follows:

$$b_k = E\left[e^{-T\sum_{j=k}^N 1_{[X_{(k)}, (1+\gamma)X_{(k)}]}(X_{(j)}) X_{(j)}}\right] \quad (4.10)$$

where the indicator function is defined as:

$$1_{[x,a]}(X_{(j)}) = \begin{cases} 1 & x \leq X_{(j)} \leq a \\ 0 & X_{(j)} > a. \end{cases} \quad (4.11)$$

We should keep in mind that in our case  $a = (1 + \gamma)X_{(k)}$  (see (4.10)). Conditioning on the random variable  $X_{(k)}$  and using the result  $E[E[X|Y]]$ , equation (??) can be

rewritten as

$$b_k = E \left[ E \left[ e^{-T \sum_{j=k}^N 1_{\{X_{(k)}, (1+\gamma)X_{(k)}\}}(X_{(j)}) X_{(j)}} | X_{(k)} \right] \right] \quad (4.12)$$

Letting the random variable  $X_{(k)} = x$ ,

$$b_k = \int_0^\infty E \left[ e^{-T \sum_{j=k}^N 1_{\{x, (1+\gamma)x\}}(X_{(j)}) X_{(j)}} | X_{(k)} = x \right] f_{X_{(k)}}(x) dx. \quad (4.13)$$

Simplifying further,

$$\begin{aligned} b_k &= \int_0^\infty e^{-Tx} E \left[ e^{-T \sum_{j=k+1}^N 1_{\{x, (1+\gamma)x\}}(X_{(j)}) X_{(j)}} | X_{(k)} = x \right] f_{X_{(k)}}(x) dx \\ &= E \left[ e^{-TX_{(k)}} E \left[ e^{-T \sum_{j=k+1}^N 1_{\{X_{(k)}, (1+\gamma)X_{(k)}\}}(X_{(j)}) X_{(j)}} | X_{(k)} \right] \right]. \end{aligned} \quad (4.14)$$

Here we introduce a notation that will greatly facilitate the derivation:

*Definition:*

$$V_k^a(X_k) = E \left[ e^{-T \sum_{j=k+1}^N 1_{\{X_{(k)}, a\}}(X_{(j)}) X_{(j)}} | X_{(k)} \right]. \quad (4.15)$$

Thus, using equations (4.14) and (4.15) we can express  $b_k$  in a compact form as follows:

$$b_k = E \left[ e^{-TX_{(k)}} V_k^{(1+\gamma)X_{(k)}}(X_{(k)}) \right]. \quad (4.16)$$

Here, we point out that the subscript of  $b$  and  $V$  is one less than the index of summation in equation (4.15), which means that the index of the smallest order statistic that falls in the window is equal to the index of  $b$ . In other words,  $b_j$  is the false alarm probability when the smallest sample that falls in the window is  $X_{(j)}$ . The rest of the calculations that will lead to the closed form expression for  $b_k$  depends on the most important observation that for  $r < s$

$$f_{X_{(s)} | X_{(r)}=x_{(r)}, X_{(r-1)}=x_{(r-1)}, \dots, X_{(1)}=x_{(1)}}(y) = f_{X_{(s)} | X_{(r)}=x_{(r)}}(y) \quad (4.17)$$

which establishes that the order statistics in a sample from a continuous distribution form a *Markov Chain* (see [8, page 20] for the proof). Using this fact, we can simplify equation (4.15) further by conditioning on  $X_{(k+1)}$ .

$$V_k^a(x) = E \left[ E \left[ e^{-T \sum_{j=k+1}^N 1_{[x,a]}(X_{(j)}) X_{(j)}} \mid X_{(k+1)}, X_{(k)} = x \right] \right] \quad (4.18)$$

$$= \int_x^\infty E \left[ e^{-T \sum_{j=k+1}^N 1_{[x,a]}(X_{(j)}) X_{(j)}} \mid X_{(k+1)} = y, X_{(k)} = x \right] \\ \times f_{X_{(k+1)} | X_{(k)}}(y/x) dy \quad (4.19)$$

Now, we observe that either  $x \leq y < a$  or  $a \leq y < \infty$ . When  $x \leq y < a$ , the indicator function equals 1. In the latter case, the indicator function is equal to 0 and thus the argument of the summation in the equation (4.19) is 0. Since the first term of the summation  $X_{(k+1)}$  is not a random variable, it can be taken out of the expectation and we obtain

$$V_k^a(x) = \int_x^a e^{-Ty} E \left[ e^{-T \sum_{j=k+2}^N 1_{[x,a]}(X_{(j)}) X_{(j)}} \mid X_{(k+1)} = y, X_{(k)} = x \right] \\ \times f_{X_{(k+1)} | X_{(k)}}(y/x) dy + \int_a^\infty f_{X_{(k+1)} | X_{(k)}}(y/x) dy \quad (4.20)$$

$$= \int_x^a e^{-Ty} \underbrace{E \left[ e^{-T \sum_{j=k+2}^N 1_{[y,a]}(X_{(j)}) X_{(j)}} \mid X_{(k+1)} = y \right]}_{V_{k+1}^a(y)} \\ \times f_{X_{(k+1)} | X_{(k)}}(y/x) dy + \int_a^\infty f_{X_{(k+1)} | X_{(k)}}(y/x) dy \quad (4.21)$$

where we used the Markov property (see (4.17)) to go from the first equality to the second. The conditional pdf of  $X_{(k+1)}$  given  $X_{(k)} = x$  for  $x \leq y$  can easily be calculated (see [8, equation 2.7.1] for details). Thus, for the exponential clutter,

$$f_{X_{(k+1)} | X_{(k)}}(y/x) = \begin{cases} (N-k)e^{-(N-k)(y-x)} & y \geq x \\ 0 & \text{otherwise.} \end{cases} \quad (4.22)$$

Substitution of equation (4.22) into equation (4.20) yields:

$$\begin{aligned}
 V_k^a(x) &= \int_a^\infty (N-k)e^{-(N-k)(y-x)} dy \\
 &\quad + \int_x^a e^{-Ty} V_{k+1}^a(y) (N-k)e^{-(N-k)(y-x)} dy \\
 &= e^{-(N-k)(a-x)} \\
 &\quad + e^{(N-k)x} \int_x^a (N-k)e^{-y[N-k+T]} V_{k+1}^a(y) dy. \tag{4.23}
 \end{aligned}$$

Now, we start processing:

If  $k = N - 1$  in expression (4.23), then,

$$V_{N-1}^a(x) = e^{-(a-x)} + e^x \int_x^a e^{-y(1+T)} V_N^a(y) dy \tag{4.24}$$

$$= e^{-(a-x)} + \frac{e^{-(a-x)} e^{-aT}}{(1+T)} [e^{(1+T)(a-x)} - 1]. \tag{4.25}$$

Substitution of equation (4.25) into equation (4.16) with  $k = N - 1$ ,  $a = (1 + \gamma)X_{(k)}$  and  $x = X_{(k)}$  results in

$$b_{N-1} = E \left\{ e^{-TX_{(k)}} V_{N-1}^{(1+\gamma)X_{(k)}}(X_{(k)}) \right\} \tag{4.26}$$

$$= E \left\{ e^{-X_{(k)}(\gamma+T)} + \frac{e^{-2TX_{(k)}} - e^{-(\gamma+2T+\gamma T)X_{(k)}}}{(1+T)} \right\}. \tag{4.27}$$

Let  $E[e^{-\beta X_{(k)}}] = M_{X_{(k)}}(\beta)$ , which is the moment generating function of  $X_{(k)}$  (see [15] for more on moment generating functions.) The derivation of  $M_{X_{(k)}}(\beta)$  is straight forward:

$$M_{X_{(k)}}(\beta) = \int_0^\infty e^{-\beta x} f_{X_{(k)}}(x) dx \tag{4.28}$$

$$= \frac{N!}{(N-k)!(k-1)!} \int_0^\infty (1 - e^{-x})^{k-1} e^{-x(N-k+1+\beta)} dx \tag{4.29}$$

and making change of variable  $1 - e^{-x} = u$  in (4.29) gives:

$$M_{X_{(k)}}(\beta) = \frac{N!}{(N-k)!(k-1)!} \int_0^1 u^{k-1} (1-u)^{N-k+\beta} du$$

$$\begin{aligned}
&= \frac{N! \Gamma(N - k + \beta + 1)}{(N - k)! \Gamma(N + \beta + 1)} \\
&= \frac{N!}{(N - k)! (N + \beta)(N + \beta - 1) \cdots (N + \beta + 1 - k)} \\
&= \frac{N!}{(N - k)!} \prod_{i=0}^{k-1} \frac{1}{(N + \beta - i)}. \tag{4.30}
\end{aligned}$$

Thus, we can express  $b_{N-1}$  in terms of the moment generating function of  $X_{(N-1)}$ :

$$b_{N-1} = M_{X_{(N-1)}}(T + \gamma) + \frac{1}{(1 + T)} \left\{ M_{X_{(N-1)}}(2T) - M_{X_{(N-1)}}(\gamma + 2T + \gamma T) \right\} \tag{4.31}$$

Similarly, by back substitution we can derive  $b_{N-2}, \dots, b_1$  in the given order. Expressions for  $b_{N-2}, \dots, b_{N-5}$  are given in the Appendix B. By looking at these expressions we realize a pattern that the expressions for  $b_k$  follows. This leads to a closed form expression for the false alarm rate,  $P_{fa}$  for any value of  $k$ ,  $1 \leq k \leq N$ .

$$P_{fa} = b_{N-j} = \sum_{i_1=0}^j \frac{\binom{j}{i_1}}{(T+1)^{i_1}} \left[ \sum_{i_2=0}^{i_1} \binom{i_1}{i_2} (-1)^{i_2} M(\beta) \right] \tag{4.32}$$

where  $\beta = (j - i_1 + i_2)\gamma + T[(i_1 + 1) + i_2\gamma]$  and  $k = N - j$  or  $j = N - k$ . Also, by using the definition (2.9) given in chapter 2 it is straight forward to derive the general expression for ADT:

$$\begin{aligned}
ADT = & T \sum_{i_1=0}^j \binom{j}{i_1} \left[ \sum_{i_2=0}^{i_1} \binom{i_1}{i_2} (-1)^{i_2} M[(j - i_1 + i_2)\gamma] \right. \\
& \left. \times \{D[(j - i_1 + i_2)\gamma][i_1 + 1 + i_2\gamma] + i_1\} \right] \tag{4.33}
\end{aligned}$$

where  $M(\beta)$  is as defined in (4.29), and  $D(\beta) = \sum_{i=0}^{k-1} \frac{1}{(N+\beta-i)}$  and  $j = N - k$ . Of course the  $P_{fa}$  and the ADT expressions given above are for the un-normalized  $Z$ , i.e., for  $\eta(K_2) = 1$ . Notice that  $i_1 + 1$  is the number of terms that form the sum  $Z$ , i.e.,  $i_1 + 1 = K_2 - k + 1$ . Thus,  $\eta(K_2) = 1/(i_1 + 1)$ . Let  $Z_{Normalized} = \bar{Z}$ , then  $\bar{Z} = \eta(K_2)Z$ . Since Threshold is equal in both cases,  $T = \eta(K_2)\bar{T}$ . Thus, we can



replace  $T$  in expression (4.32) by  $\bar{T}/(i_1 + 1)$  in order to obtain the normalized  $P_{fa}$  expression, i.e.,

$$P_{fa} = b_{N-j} = \sum_{i_1=0}^j \frac{\binom{j}{i_1}}{(\bar{T}/(i_1 + 1) + 1)^{i_1}} \left[ \sum_{i_2=0}^{i_1} \binom{i_1}{i_2} (-1)^{i_2} M(\beta) \right] \quad (4.34)$$

where  $\beta = (j - i_1 + i_2)\gamma + \bar{T}[(i_1 + 1) + i_2\gamma]$  and  $k = N - j$  or  $j = N - k$ . The following normalized ADT expression is derived as before to be

$$ADT = \bar{T} \sum_{i_1=0}^j \frac{\binom{j}{i_1}}{(i_1 + 1)} \left[ \sum_{i_2=0}^{i_1} \binom{i_1}{i_2} (-1)^{i_2} M[(j - i_1 + i_2)\gamma] \times \{D[(j - i_1 + i_2)\gamma][i_1 + 1 + i_2\gamma] + i_1\} \right] \quad (4.35)$$

where  $M(\beta)$  is as defined in (4.29) and  $D(\beta) = \sum_{i=0}^{k-1} \frac{1}{(N+\beta-i)}$  and  $j = N - k$ .

## Chapter 5

### DISCUSSION OF RESULTS

At the end of the thesis we present some results to facilitate the comparison of the VTM-CFAR detector with those detectors that are well known to have good performance characteristics under clutter power transitions or multiple target situation. In addition to presenting tables we have plotted various performance curves in order to obtain a better feel for the comparisons. The constant scale factor,  $T$ , the average detection threshold, ADT and other performance values in homogeneous background are obtained analytically. The performance characteristics at clutter power transitions and in presence of multiple targets are obtained by Monte Carlo Simulation with  $10^6$  runs. In Figures 1-5, we show the block diagrams of the processors mentioned in the previous chapters.

In Figures 6,7, and 8,  $k$  vs. ADT are plotted for selected  $\gamma$  values. In Figure 6 we observe that the VTM with  $k = 20, 21$  and  $\gamma = 2.0$  performs closest to the OS detector with  $k = 20, 21$  in terms of ADT. Thus, we can expect the two detectors to have similar detection performances in presence of homogeneous noise. Comparing Figure 6 with Figure 7, we observe that for bigger design  $P_{fa}$ 's the VTM-CFAR with  $\gamma = 2.0$  and  $k \leq 21$  has smaller ADT values. A careful inspection of Figure 8 reveals that for  $N = 16$ , and  $P_{fa} = 0.001$  the VTM-CFAR performs worse than the OS-CFAR in

terms of ADT, which implies that the VTM-CFAR becomes superior to the OS-CFAR as the window size gets larger. The results demonstrate that some improvement in the overall performance can be achieved by using a VTM-CFAR detector with proper design parameters. For example, if the VTM detector with  $k = 20, \gamma = 1.0$  is employed with  $N = 24$ , then, it will operate close to the optimum OS detector in regions of clutter power transitions (see Tables 6 and 7). However, the VTM detector with  $k = 20$  and  $\gamma = 1.0$  is superior to the OS detector with  $k = 21$  in multiple target situations (see Tables 4 and 5). Figure 9 shows the detection performance in homogeneous background of the OS and the VTM-CFAR processors as a function of the primary target SNR at  $P_{fa} = 10^{-3}$  for a window size of  $N = 24$ . As predicted from the ADT characteristics, Figure 9 indicates that the OS with  $k \approx 21, 20$  and the VTM with  $k = 20, 21; \gamma = 2.0$  are very close; note that the VTM with  $k = 20$  and  $\gamma = 1.0$  suffers some detection loss in homogeneous background. A careful inspection of Figure 9 also reveals that the  $P_d$  characteristic for the VTM with  $k = 21, \gamma = 1$  is reasonably close to the  $P_d$  characteristic of the OS processor with  $k = 20, k = 21$ . In Figure 10, comparison of detection performance in presence of four interfering targets,  $INR/SNR = 1$ , of the OS-CFAR with  $k = 21$  and the VTM with  $k = 21, \gamma = 1$  or  $2; k = 20, \gamma = 1$  or  $2$  is shown. Clearly, the VTM with  $k = 20, \gamma = 1$  or  $2$  are superior to the CA, and the OS with  $k = 21$  in terms of detection probability in presence of multiple targets. Figures 11, 12, and 13 show false alarm rate performance of the SO-, the GO- and the VTM-CFAR detectors. From these Figures we see clearly that the VTM-CFAR with  $k = 21, \gamma = 1$  or  $2; k = 20, \gamma = 2$  are superior to the OS with  $k = 21$  and that their performance does not degrade as much as the OS with  $k = 21$  as CNR increases.

All in all, comparing all the Tables and performance curves given, we see that the VTM detector with  $k = 20$ ,  $\gamma = 2.0$  is the best detector; and the second best VTM detector is the one with  $k = 20$ ,  $\gamma = 1.0$ . Actually, these two VTM detectors have very close performance. The VTM with  $k = 20$  and  $\gamma = 1.0$  has slightly superior performance in multiple targets situation; whereas the VTM detector with  $k = 20$  and  $\gamma = 2.0$  is superior in clutter power transitions.

### 5.1 Areas For Further Research

The results shown above were obtained for exponentially distributed clutter. Further study is required with clutter distributions having lighter tails than the exponential distribution. In particular, if a linear detector is used instead of the square-law detector, the range samples from the clutter regions would be governed by the Rayleigh distribution. Here the variable trimming along with the averaging operation incorporated in the VTM detector may give better performance than the OS-CFAR detector. More generally, other clutter models need to be considered to determine the overall effectiveness of this scheme.

Recently published literature [11,12,14] indicate that there is much interest in CFAR detection in the radar research community.

## Chapter 6

# CONCLUSIONS

Previously published results established the usefulness of the Modified Trimmed Mean filter in restoration of nonstationary signals embedded in additive noise with impulsive components. Our original motivation in this study was to investigate the usefulness of this technique for CFAR radar detection, since radar detection under clutter power transitions and multiple target situations is a related problem. In particular, we modified the MTM filtering technique according to the specifics of the CFAR radar detection problem; and we called the resulting detector the Variably Trimmed Mean (VTM) detector.

The results obtained validate our predictions that this new technique, with properly chosen design parameters, offers some improvement over the previously known techniques in the presence of clutter power transitions and multiple targets.

The mentioned improvement occurs due to the fact that the new technique employed combines the merits of using ordered statistics with averaging and censoring, in addition to estimating the threshold data adaptively. This is the main reason of the superior performance of this technique as opposed to the previously known ones in CFAR detection.

However, it should be noted that, for small window size, the VTM-CFAR detector does not perform better than the OS detector in homogeneous background. An important limitation of this new technique is the absence of analytical expressions for probability of false alarm under clutter power transitions and for probability of detection in presence of multiple targets. Obviously, this dictates the use of simulations for evaluating the performance characteristics of this new detector.

It is expected that the VTM-CFAR scheme presented may prove to be useful for CFAR radar detection for non-homogeneous background. Another potential application area of the presented new technique may be in sonar detection in the presence of impulsive noise.

## Appendix A

### Proof of Proposition 1

In this appendix we prove proposition 1 given earlier in chapter 4.

**Proof:** Let us define random variables  $V_i = X_i/\mu, i = 1, \dots, N$ . Then, since  $\mu$  is a scale parameter of  $f_{\mathbf{X}}(\mathbf{x}; \mu, \underline{\theta})$ , the joint pdf  $f_{\mathbf{V}}(\mathbf{v}; \mu, \underline{\theta})$  of  $\mathbf{V}$  given by (see Definition 2)

$$f_{\mathbf{V}}(\mathbf{v}; \mu, \underline{\theta}) = g(\mathbf{v}; \underline{\theta}) \quad (\text{A.1})$$

is independent of  $\mu$ . In addition, for each scale invariant event  $A_i(\mathbf{X}), i = 1, \dots, m$ , the following relations hold:

$$A_i(\mathbf{X}) = A_i(\mathbf{V}), i = 1, \dots, m. \quad (\text{A.2})$$

We therefore have

$$\begin{aligned} P[A_1(\mathbf{X}), A_2(\mathbf{X}), \dots, A_m(\mathbf{X})] &= \underbrace{\int_{x_1} \int_{x_2} \dots \int_{x_N}}_{A_1(\mathbf{X}) \times A_2(\mathbf{X}) \times \dots \times A_m(\mathbf{X})} f_{\mathbf{X}}(\mathbf{x}; \mu, \underline{\theta}) d\mathbf{x} \\ &= \underbrace{\int_{v_1} \int_{v_2} \dots \int_{v_N}}_{A_1(\mathbf{V}) \times A_2(\mathbf{V}) \times \dots \times A_m(\mathbf{V})} g(\mathbf{v}; \underline{\theta}) d\mathbf{v} \quad (\text{A.3}) \end{aligned}$$

where  $\times$  denotes the cartesian product. The proof is complete since the right hand side of expression (A.3) is independent of  $\mu$ .

## Appendix B

### Derivation of $P_{fa}$ for VTM-CFAR Processor

In this appendix, the derivation of the false alarm probability of the adaptive-VTM CFAR processor is given. The argument used in this derivation is similar to that employed in deriving the false alarm probability,  $b_{N-1}$ , when  $k = N - 1$ . From equation (4.16)

$$b_{N-2} = E \left\{ e^{-TX_{(k)}} V_{N-2}^{(1+\gamma)X_{(k)}}(X_{(k)}) \right\} \quad (\text{B.1})$$

and using equation (4.23) with  $k = N - 2$ , we get:

$$V_{N-2}^a(x) = e^{-2(a-x)} + e^{2x} \int_x^a 2 e^{-y(2+T)} V_{N-1}^a(y) dy \quad (\text{B.2})$$

Substitution of expression (4.25) in (B.2) yields:

$$\begin{aligned} V_{N-2}^a(x) = & e^{-2(a-x)} + 2e^{-2(a-x)}e^{-aT} \left\{ \frac{(e^{(T+1)(a-x)} - 1)}{(T+1)} \right. \\ & + \frac{e^{-aT}}{2(T+1)^2} (e^{2(T+1)(a-x)} - 1) \\ & \left. - \frac{e^{-aT}}{(T+1)^2} (e^{(T+1)(a-x)} - 1) \right\} \quad (\text{B.3}) \end{aligned}$$

Substitution of equation (B.3) into equation (B.1) with  $a = (1 + \gamma)X_k$  and  $x = X_k$  into (B.3) results in

$$\begin{aligned} b_{N-2} = & E \left\{ e^{-(2\gamma+T)X_{(k)}} + \frac{2}{(T+1)} \left[ e^{-(\gamma+2T)X_{(k)}} + e^{-(2\gamma+(2+\gamma)T)X_{(k)}} \right] \right. \\ & \left. + \frac{1}{(T+1)^2} \left[ e^{-3TX_{(k)}} - e^{-(\gamma+(3+\gamma)T)X_{(k)}} + e^{-(2\gamma+(3+2\gamma)T)X_{(k)}} \right] \right\} \quad (\text{B.4}) \end{aligned}$$



In above equation we emphasize that  $k = N - 2$ . Now, it is obvious that  $b_{N-2}$  can be expressed in terms of the moment generating function of  $X_{(k)}$ . For simplicity we refer to the moment generating function  $M_{X_{(k)}}$  by  $M$  and proper  $k$  value will be understood from the context.

$$b_{N-2} = M(2\gamma + T) + \frac{2}{(T+1)} [M(\gamma + 2T) - M(2\gamma + (2 + \gamma)T)] \\ + \frac{1}{(T+1)^2} [M(3T) - 2M(\gamma + (3 + \gamma)T) + M(2\gamma + (3 + 2\gamma)T)] \quad (B.5)$$

We continue in exactly the same way to iterate the solution by back substitution.

$$b_{N-3} = E \left\{ e^{-TX_{(k)}} V_{N-3}^{(1+\gamma)X_{(k)}}(X_{(k)}) \right\} \quad (B.6)$$

$$V_{N-3}^a(x) = e^{-3(a-x)} + 3e^{-3(a-x)}e^{-aT} \left\{ \frac{(e^{(T+1)(a-x)} - 1)}{(T+1)} \right. \\ + \frac{2e^{-aT}}{(T+1)^2} \left[ \frac{1}{2}e^{2(T+1)(a-x)} - e^{(T+1)(a-x)} + \frac{1}{2} \right] \\ \left. + \frac{e^{-2aT}}{(T+1)^3} \left[ \frac{1}{3}(e^{3(T+1)(a-x)} - e^{2(T+1)(a-x)} + e^{(T+1)(a-x)} - \frac{1}{3}) \right] \right\} \quad (B.7)$$

Thus, substituting (B.7) into (B.6) with  $x = X_{(k)}$  and  $a = (1 + \gamma)X_{(k)}$  gives,

$$b_{N-3} = M(3\gamma + T) \\ + \frac{3}{(T+1)} [M(2\gamma + 2T) - M(3\gamma + (2 + \gamma)T)] \\ + \frac{3}{(T+1)^2} [M(\gamma + 3T) - 2M(2\gamma + (3 + \gamma)T) + M(3\gamma + (3 + 2\gamma)T)] \\ + \frac{1}{(T+1)^3} [M(4T) - 3M(\gamma + (4 + \gamma)T)] \\ + 3M(2\gamma + (2 + \gamma)2T) - M(3\gamma + (4 + 3\gamma)T)] \quad (B.8)$$

The false alarm probability for  $k=N-4$  is found by using

$$b_{N-4} = E \left\{ e^{-TX_{(k)}} V_{N-4}^{(1+\gamma)X_{(k)}}(X_{(k)}) \right\} \quad (B.9)$$

Back substituting (B.7) into (4.25) and evaluating results in

$$\begin{aligned}
V_{N-4}^a(x) = & e^{-4(a-x)} + e^{-4(a-x)} e^{-2aT} \left\{ \frac{4e^{aT} (e^{(T+1)(a-x)} - 1)}{(T+1)} \right. \\
& + \frac{6}{(T+1)^2} [e^{2(T+1)(a-x)} - 2e^{(T+1)(a-x)} + 1] \\
& + \frac{4e^{-aT}}{(T+1)^3} [e^{3(T+1)(a-x)} - 3e^{2(T+1)(a-x)} + 3e^{(T+1)(a-x)} - 1] \\
& + \frac{e^{-2aT}}{(T+1)^4} [e^{4(T+1)(a-x)} - 4e^{3(T+1)(a-x)} \\
& \left. + 6e^{2(T+1)(a-x)} - 4e^{(T+1)(a-x)} + 1] \right\} \quad (B.10)
\end{aligned}$$

which when substituted into  $b_{N-4}$  with  $x = X_{(k)}$  and  $a = (1 + \gamma)X_{(k)}$  gives us the  $P_{fa}$  for  $k = N - 4$  i.e.,

$$\begin{aligned}
b_{N-4} = & M(4\gamma + T) + \frac{4}{(T+1)} [M(3\gamma + 2T) - 4M(4\gamma + (2 + \gamma)T)] \\
& + \frac{6}{(T+1)^2} [M(2\gamma + 3T) - 2M(3\gamma + (3 + \gamma)T) + M(4\gamma + (3 + 2\gamma)T)] \\
& + \frac{4}{(T+1)^3} [M(\gamma + 4T) - 3M(2\gamma + (4 + \gamma)T) \\
& + 3M(3\gamma + (4 + 2\gamma)T) - M(4\gamma + T(4 + 3\gamma))] \\
& + \frac{1}{(T+1)^4} [M(5T) - 4M(\gamma + (5 + \gamma)T) + 6M(2\gamma + (5 + 2\gamma)T) \\
& - 4M(3\gamma + (5 + 3\gamma)T) + M(4\gamma + (5 + 4\gamma)T)] \quad (B.11)
\end{aligned}$$

The  $P_{fa}$  for  $k = N - 5$  is computed in exactly the same way.

$$b_{N-5} = E \left\{ e^{-TX_{(k)}} V_{N-5}^{(1+\gamma)X_{(k)}}(X_{(k)}) \right\} \quad (B.12)$$

$$\begin{aligned}
V_{N-5}^a(x) = & e^{-5(a-x)} + e^{-5(a-x)} e^{-2aT} \left\{ \frac{5e^{aT} (e^{(T+1)(a-x)} - 1)}{(T+1)} \right. \\
& + \frac{10}{(T+1)^2} [e^{2(T+1)(a-x)} - 2e^{(T+1)(a-x)} + 1] \\
& + \frac{10e^{-aT}}{(T+1)^3} [e^{3(T+1)(a-x)} - 3e^{2(T+1)(a-x)} + 3e^{(T+1)(a-x)} - 1] \\
& \left. + \frac{e^{-2aT}}{(T+1)^4} [e^{4(T+1)(a-x)} - 4e^{3(T+1)(a-x)} + 6e^{2(T+1)(a-x)} - 4e^{(T+1)(a-x)} + 1] \right\}
\end{aligned}$$

$$\begin{aligned}
& + \frac{5e^{-2aT}}{(T+1)^4} \left[ e^{4(T+1)(a-z)} - 4e^{3(T+1)(a-z)} \right. \\
& + 6e^{2(T+1)(a-z)} - 4e^{(T+1)(a-z)} + 1 \left. \right] \\
& + \frac{e^{-3aT}}{(T+1)^5} \left[ e^{5(T+1)(a-z)} - 5e^{4(T+1)(a-z)} + 10e^{3(T+1)(a-z)} \right. \\
& \left. - 10e^{2(T+1)(a-z)} + 5e^{(T+1)(a-z)} - 1 \right] \left. \right\} \quad (B.13)
\end{aligned}$$

Thus,

$$\begin{aligned}
b_{N-5} = & M(5\gamma + T) + \frac{5}{(T+1)} [M(4\gamma + 2T) - 5M(5\gamma + (2 + \gamma)T)] \\
& + \frac{10}{(T+1)^2} [M(3\gamma + 3T) - 2M(4\gamma + (3 + \gamma)T) + M(5\gamma + (3 + 2\gamma)T)] \\
& + \frac{10}{(T+1)^3} [M(2\gamma + 4T) - 3M(3\gamma + (4 + \gamma)T) \\
& + 3M(4\gamma + (4 + 2\gamma)T) - M(5\gamma + T(4 + 3\gamma))] \\
& + \frac{5}{(T+1)^4} [M(\gamma + 5T) - 4M(2\gamma + (5 + \gamma)T) + 6M(2\gamma + (5 + 2\gamma)T) \\
& - 4M(4\gamma + (5 + 3\gamma)T) + M(5\gamma + (5 + 4\gamma)T)] \\
& + \frac{1}{(T+1)^5} [M(6T) - 5M(\gamma + (6 + \gamma)T) + 10M(2\gamma + (6 + 2\gamma)T) \\
& - 10M(3\gamma + (6 + 3\gamma)T) + 5M(4\gamma + (6 + 4\gamma)T) \\
& - M(5\gamma + (6 + 5\gamma)T)]. \quad (B.14)
\end{aligned}$$

On examining  $b_{N-1}, \dots, b_{N-5}$  we see a pattern which leads to one  $P_{fa}$  expression for any  $k$  value.

## References

- [1] M. Weiss " Analysis of some modified cell-averaging CFAR processors in multiple-target situations ," *IEEE Transactions on Aerospace and Electronic Systems*, **AES-18**, (Jan. 1982), 102-113.
- [2] P. P. Gandhi and S. A. Kassam, " Analysis of some CFAR processors in nonhomogeneous background," *IEEE Transactions on Aerospace and Electronic Systems*, **AES-24**, (July 1988), 427-445.
- [3] H. Rohling, " Radar CFAR thresholding in clutter and multiple target situations," *IEEE Transactions on Aerospace and Electronic Systems*, **AES-19**, (July 1983), 608-621.
- [4] I. Ozgunes, P. P. Gandhi and S. A. Kassam " A CFAR detection scheme based on modified trimmed mean thresholding," *In Proc. of the Conference of Information Science and Systems*, (March 1989).
- [5] J. Ritcey, " Performance analysis of the censored mean level detector," *IEEE Transactions on Aerospace and Electronic Systems*, **AES-22**, (July 1986), 443-454.
- [6] A. C. Bovik, T. S. Huang, D. C. Munson, Jr., " A generalization of median filtering using linear combination of order statistics," *IEEE Trans. Acoust., Speech, Signal*

*Processing*, vol. ASSP-31, (December 1983), 1342-1350.

- [7] Y. H. Lee and S. A. Kassam, "Generalized median filtering and nonlinear filtering techniques," *IEEE Trans. Acoust., Speech, Signal Processing*, vol. ASSP-33, (July 1985), 672-683.
- [8] Herbert A. David, (1981) *Order Statistics*. Wiley, 1981, Second Edition.
- [9] Trunk, G. V. , Cantrell, B. V. , and Queen, F.D. (1974) "Modified generalized sign test processor for 2-D radar." *IEEE Transactions on Aerospace and Electronic Systems*, AES-10 (Sept. 1974), 574-582.
- [10] H. Goldman and I. Bar-David, "Analysis and application of the excision CFAR detector," *IEE Proceedings*, Vol. 135, Pt. F, No.6, (December 1988) 563-575.
- [11] Stephen Blake, "OS-CFAR theory for multiple targets and non-uniform clutter." *IEEE Transactions on Aerospace and Electronic Systems*, AES-6 (November 1988), 785-791.
- [12] Nadav Levanon, "Detection loss due to interfering targets in Ordered Statistics CFAR." *IEEE Transactions on Aerospace and Electronic Systems*, AES-6 (November 1988), 678-681.
- [13] P. P. Gandhi and S. A. Kassam "An adaptive order statistic constant false alarm rate detector."
- [14] Emad K. Al-Hussaini "Performance of the greater-of and censored greater-of detectors in multiple target environments." *IEE Proceedings*, Vol. 135, Pt. F. No. 3 (June 1988).

[15] Athanasios Papoulis(1984) *Probability, Random Variables, and Stochastic Processes.*

McGraw-Hill,1984,Second Edition

[16] Sheldon Ross *A First Course in Probability.* Macmillan,1976,Second Edition

## FIGURES and TABLES

Table 1 : Constant scale factor T and Average Detection Threshold of GO-CFAR Detector.

$P_{fa}$	Optimum ADT	$N = 16$		$N = 24$	
		T	ADT	T	ADT
$10^{-1}$	2.3026	0.2627	2.5145	0.1754	2.4441
$10^{-2}$	4.6052	0.5728	5.4827	0.3719	5.1816
$10^{-3}$	6.9078	0.9359	8.9577	0.5908	8.2317

Table 2 : Constant scale factor T and Average Detection Threshold of SO-CFAR Detector.

$P_{fa}$	Optimum ADT	$N = 16, k = 14$		$N = 24, k = 21$	
		T	ADT	T	ADT
$10^{-1}$	2.3026	1.3625	2.5625	1.2752	2.4771
$10^{-2}$	4.6052	3.0249	5.6891	2.7319	5.3210
$10^{-3}$	6.9078	5.0300	9.4600	4.4078	8.5627

Table 3 : Constant scale factor  $T$  and Average Detection Threshold of the VTM-CFAR Detector with  $\eta(K_2) = 1/(K_2 - k + 1)$ .

$N = 24, \text{Design } P_{fa} = 10^{-3}$			
$k$	$\gamma$	$T$	ADT
22	0.10000	3.767728	8.656557
22	0.25000	3.684335	8.741631
22	0.50000	3.514345	8.842375
22	0.75000	3.360350	8.859883
22	1.00000	3.238421	8.831052
22	2.00000	3.001415	8.679820
21	0.10000	4.373288	8.595652
21	0.25000	4.253289	8.687183
21	0.50000	4.014467	8.780179
21	0.75000	3.800912	8.784838
21	1.00000	3.631138	8.746226
21	2.00000	3.281645	8.563764
20	0.10000	5.007010	8.588369
20	0.25000	4.851740	8.683609
20	0.50000	4.547264	8.770417
20	0.75000	4.276477	8.767860
20	1.00000	4.059497	8.724521
20	2.00000	3.588250	8.517207
18	0.10000	6.435691	8.664460
18	0.25000	6.210353	8.767033
18	0.50000	5.772578	8.851266
18	0.75000	5.381757	8.844525
18	1.00000	5.062599	8.798253
18	2.00000	4.309754	8.553805
$N = 16, \text{Design } P_{fa} = 10^{-3}$			
14	0.10000	5.006803	9.494599
14	0.25000	4.918793	9.609330
14	0.50000	4.721133	9.781494
14	0.75000	4.519513	9.853190
14	1.00000	4.339345	9.841975
14	2.00000	3.889794	9.557630
13	0.10000	6.103888	9.540107
13	0.25000	5.974751	9.672779
13	0.50000	5.686565	9.859839
13	0.75000	5.392674	9.930309
13	1.00000	5.128386	9.910476
13	2.00000	4.442138	9.561359
12	0.10000	7.376223	9.676599
12	0.25000	7.206164	9.824957
12	0.50000	6.825778	10.029464
12	0.75000	6.435243	10.106696
12	1.00000	6.080349	10.087201
12	2.00000	5.121474	9.695518



Table 4 : Detection performance of the adaptive- $q$  VTM detector with  $q = X_{(k)}$ ,  $N = 24$ , design  $P_{fa} = 10^{-3}$ , four interfering targets,  $\eta(K_2) = 1/(K_2 - k + 1)$  and  $SNR = 15dB$ . Note that  $P_d = 0.258$  for the CA detector and 0.410 for the OS-CFAR detector with  $k = 21$  and 0.218 for the GO-CFAR detector.

$\gamma$ $k$	0.1	0.25	0.5	0.75	1.0	2.0
16	0.689	0.688	0.688	0.690	0.694	0.708
17	0.683	0.683	0.684	0.687	0.691	0.705
18	0.673	0.674	0.676	0.680	0.684	0.697
19	0.654	0.657	0.662	0.667	0.672	0.680
20	0.616	0.622	0.632	0.641	0.646	0.641
21	0.412	0.417	0.427	0.433	0.436	0.417
22	0.221	0.224	0.229	0.232	0.232	0.213

Table 5 : Detection performance of the adaptive- $q$  VTM detector with  $q = X_{(k)}$ ,  $N = 24$ , design  $P_{fa} = 10^{-3}$ , three interfering targets,  $\eta(K_2) = 1/(K_2 - k + 1)$  and  $SNR = 15dB$ . Note that  $P_d = 0.341$  for the CA detector and 0.643 for the OS-CFAR detector with  $k = 21$  and 0.282 for the GO-CFAR detector.

$\gamma$ $k$	0.1	0.25	0.5	0.75	1.0	2.0
17	0.711	0.709	0.709	0.711	0.714	0.726
18	0.705	0.705	0.706	0.708	0.711	0.723
19	0.696	0.697	0.698	0.702	0.706	0.715
20	0.680	0.682	0.686	0.691	0.695	0.701
21	0.644	0.649	0.659	0.667	0.671	0.665
22	0.395	0.400	0.407	0.412	0.414	0.396

Table 6: False alarm performance of the VTM-CFAR detector with  $q = X_{(k)}$ ,  $N = 24$ , design  $P_{fa} = 10^{-3}$ ,  $\eta(K_2) = 1/(K_2 - k + 1)$  and  $CNR = 10dB$  with number of clutter cells in the window = 12. Note that  $P_{fa} = 0.0212$  for the CA-CFAR detector and 0.0137 for the OS-CFAR detector with  $k = 21$  and 0.0037 for the GO-CFAR detector.

$\gamma$ $k$	0.1	0.25	0.5	0.75	1.0	2.0
17	0.0479	0.0492	0.0510	0.0514	0.0510	0.0448
18	0.0358	0.0368	0.0381	0.0384	0.0379	0.0322
19	0.0263	0.0270	0.0279	0.0280	0.0274	0.0228
20	0.0193	0.0197	0.0202	0.0203	0.0197	0.0161
21	0.0138	0.0141	0.0144	0.0143	0.0139	0.0115
22	0.0099	0.0101	0.0102	0.0102	0.0099	0.0083

Table 7: False alarm performance of the VTM-CFAR detector with  $q = X_{(k)}$ ,  $N = 24$ , design  $P_{fa} = 10^{-3}$ ,  $\eta(K_2) = 1/(K_2 - k + 1)$  and  $CNR = 15dB$  with number of clutter cells in the window = 12. Note that  $P_{fa} = 0.0243$  for the CA-CFAR detector and 0.0141 for the OS-CFAR detector with  $k = 21$  and 0.0038 for the GO-CFAR detector.

$\gamma$ $k$	0.1	0.25	0.5	0.75	1.0	2.0
17	0.0562	0.0579	0.0602	0.0611	0.0605	0.0527
18	0.0397	0.0408	0.0424	0.0426	0.0421	0.0357
19	0.0281	0.0289	0.0298	0.0299	0.0292	0.0243
20	0.0197	0.0203	0.0208	0.0208	0.0203	0.0166
21	0.0142	0.0144	0.0148	0.0148	0.0144	0.0117
22	0.010	0.0103	0.0105	0.0104	0.0102	0.0086

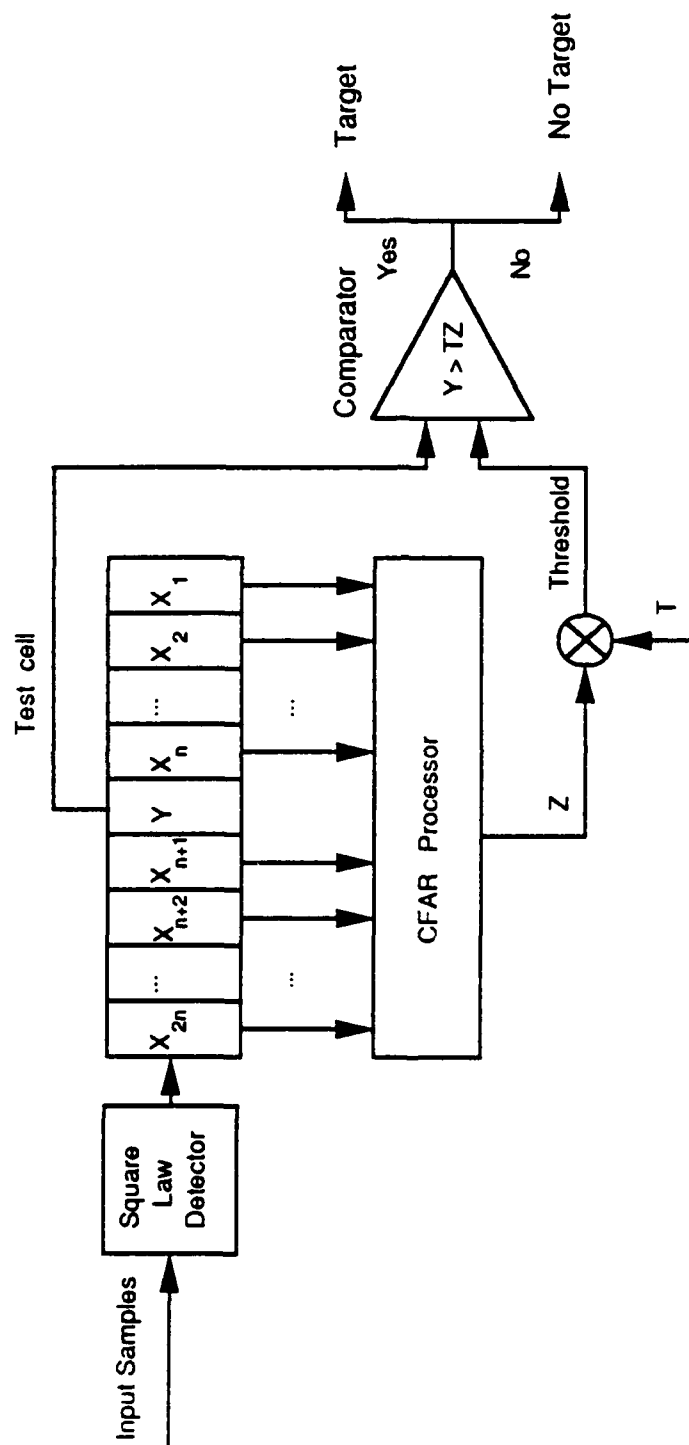


Fig. 1 Block diagram of typical CFAR processor.

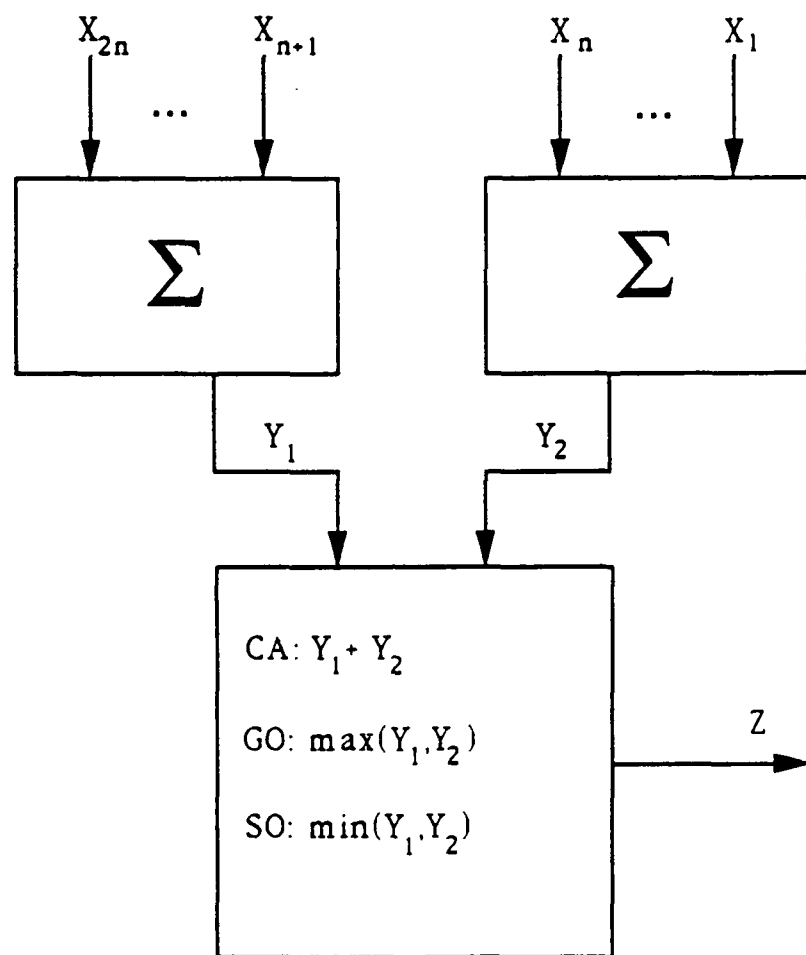


Figure 2 : Mean level CFAR Detectors.

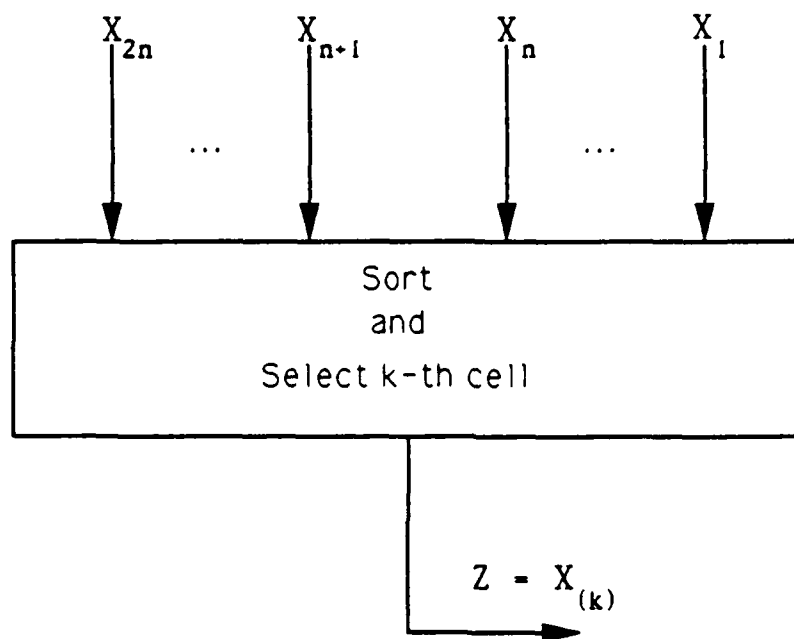


Figure 3 : Order Statistic CFAR Detector.

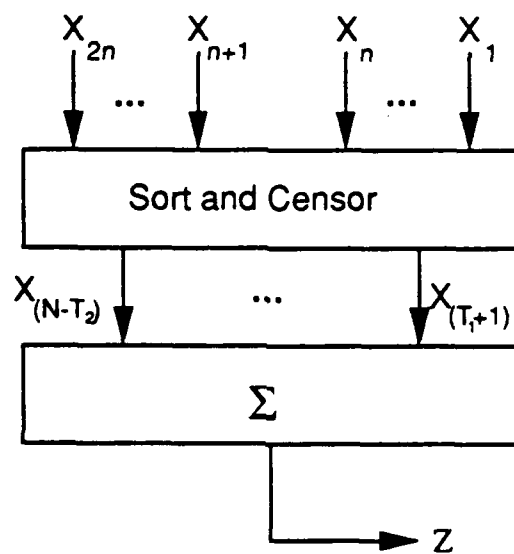


Figure 4 : Trimmed Mean CFAR Detector.

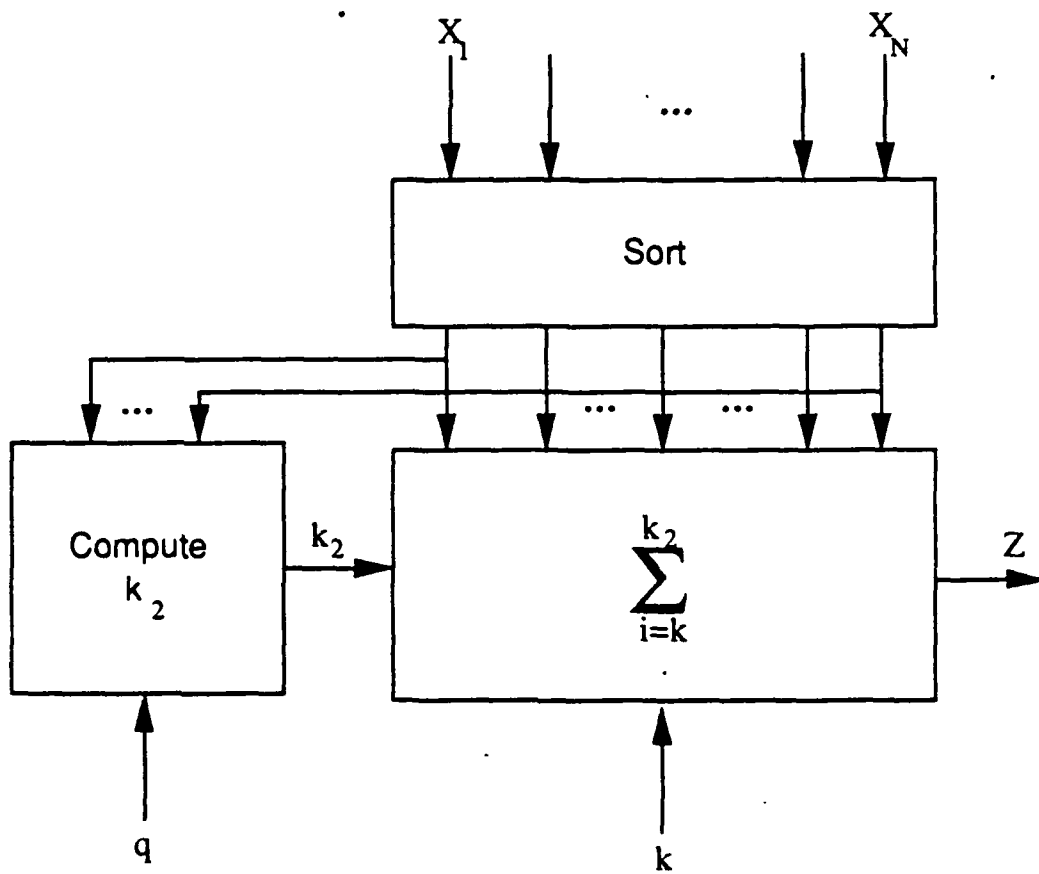


Figure 5 : Variably Trimmed Mean CFAR Detector.

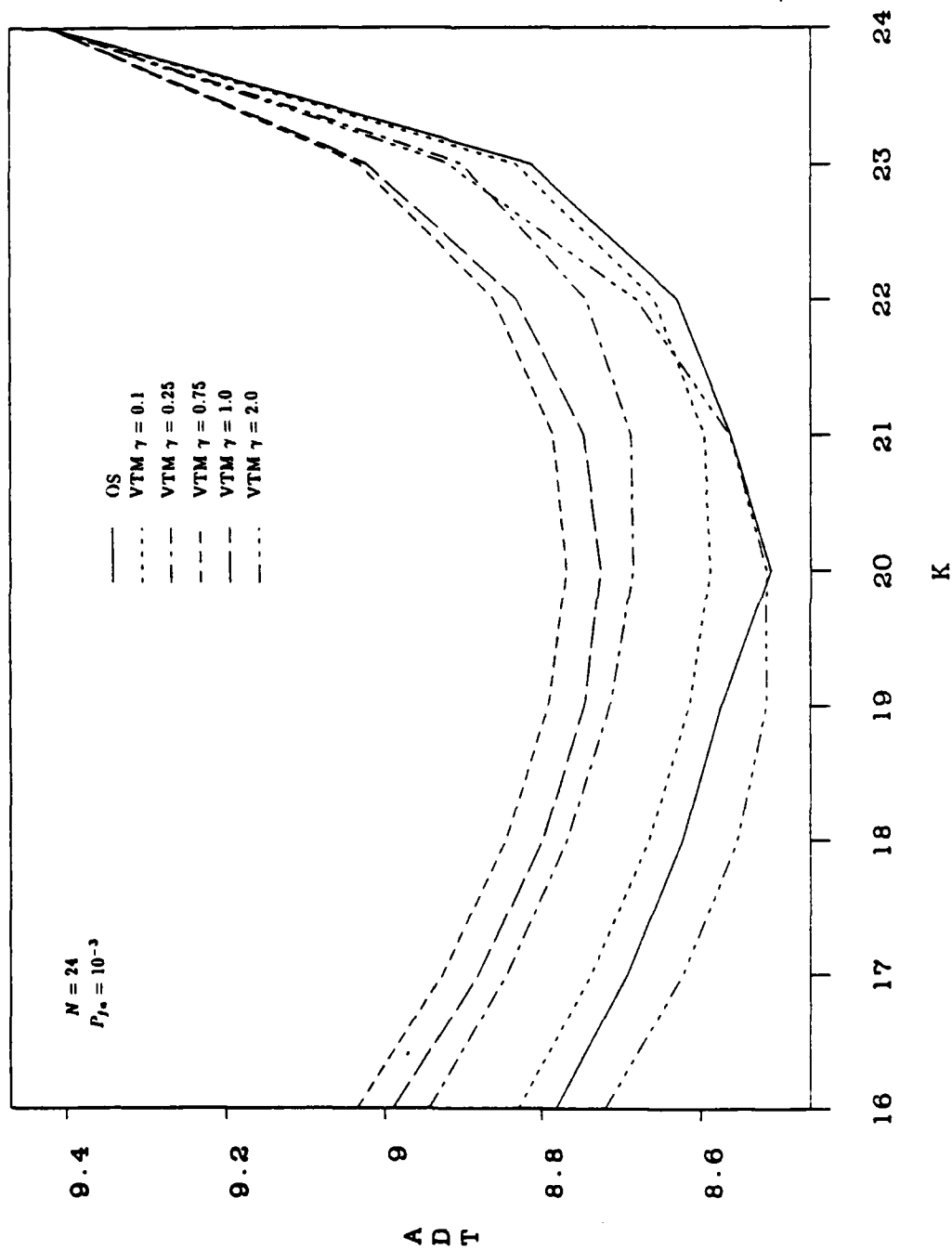


Figure 6 : The average detection threshold ADT of OS-CFAR processor and VTM-CFAR processor with selected  $\gamma$  values as a function of  $k$ .



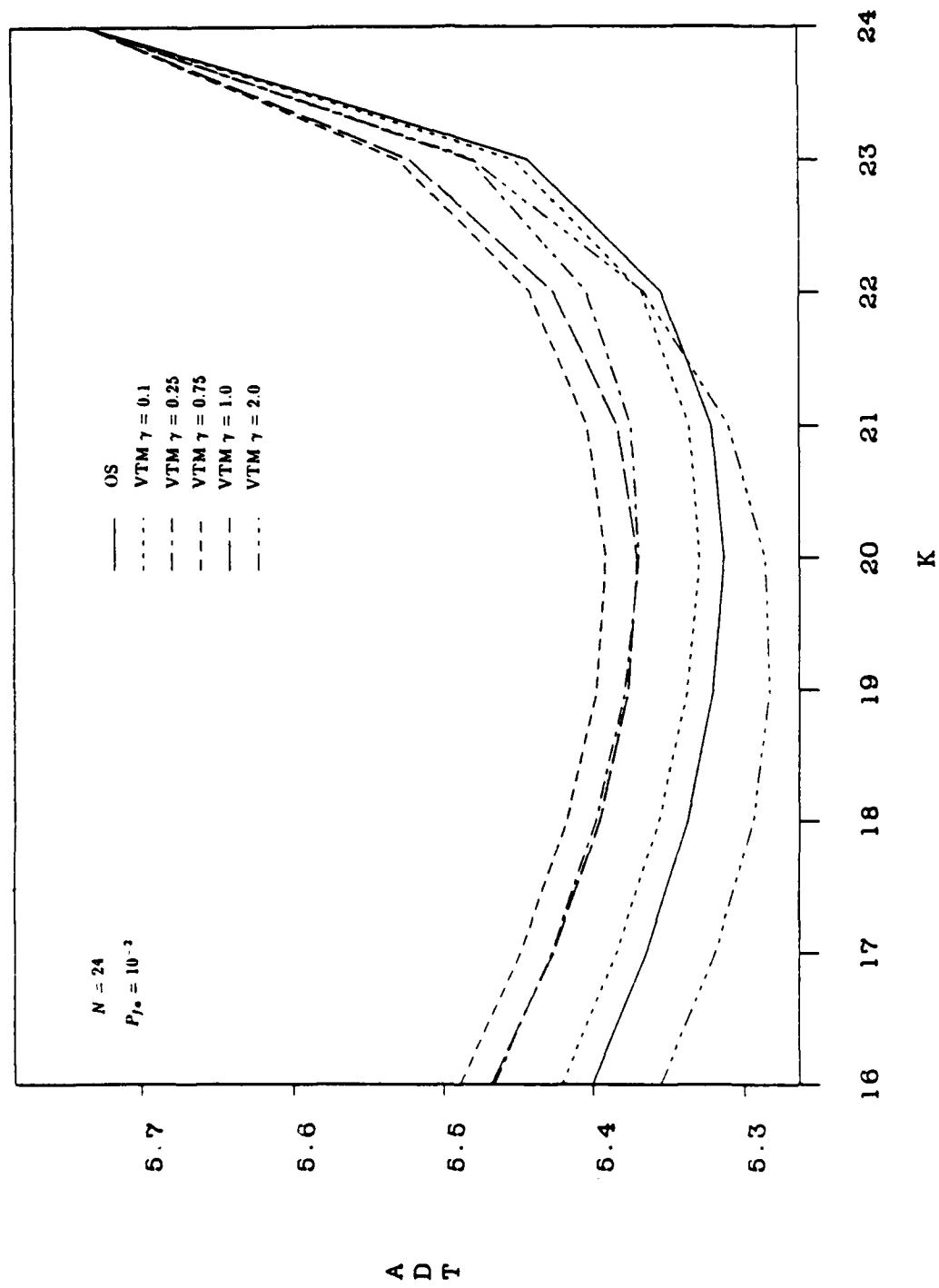


Figure 7 : The average detection threshold ADT of OS-CFAR processor and VTM-CFAR processor with selected  $\gamma$  values as a function of  $k$ .

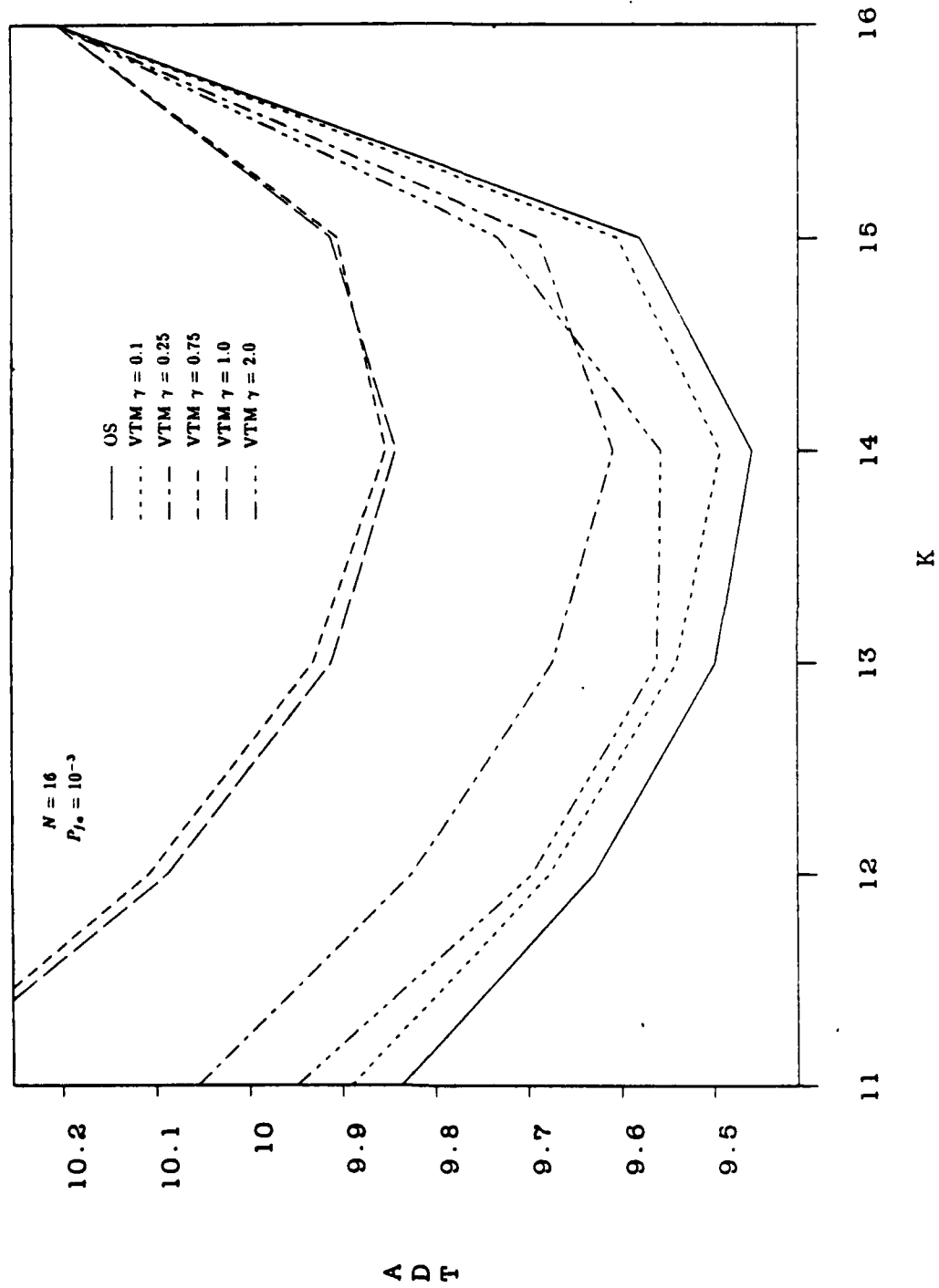


Figure 8 : The average detection threshold ADT of OS-CFAR processor and VTM-CFAR processor with selected  $\gamma$  values as a function of  $k$ .

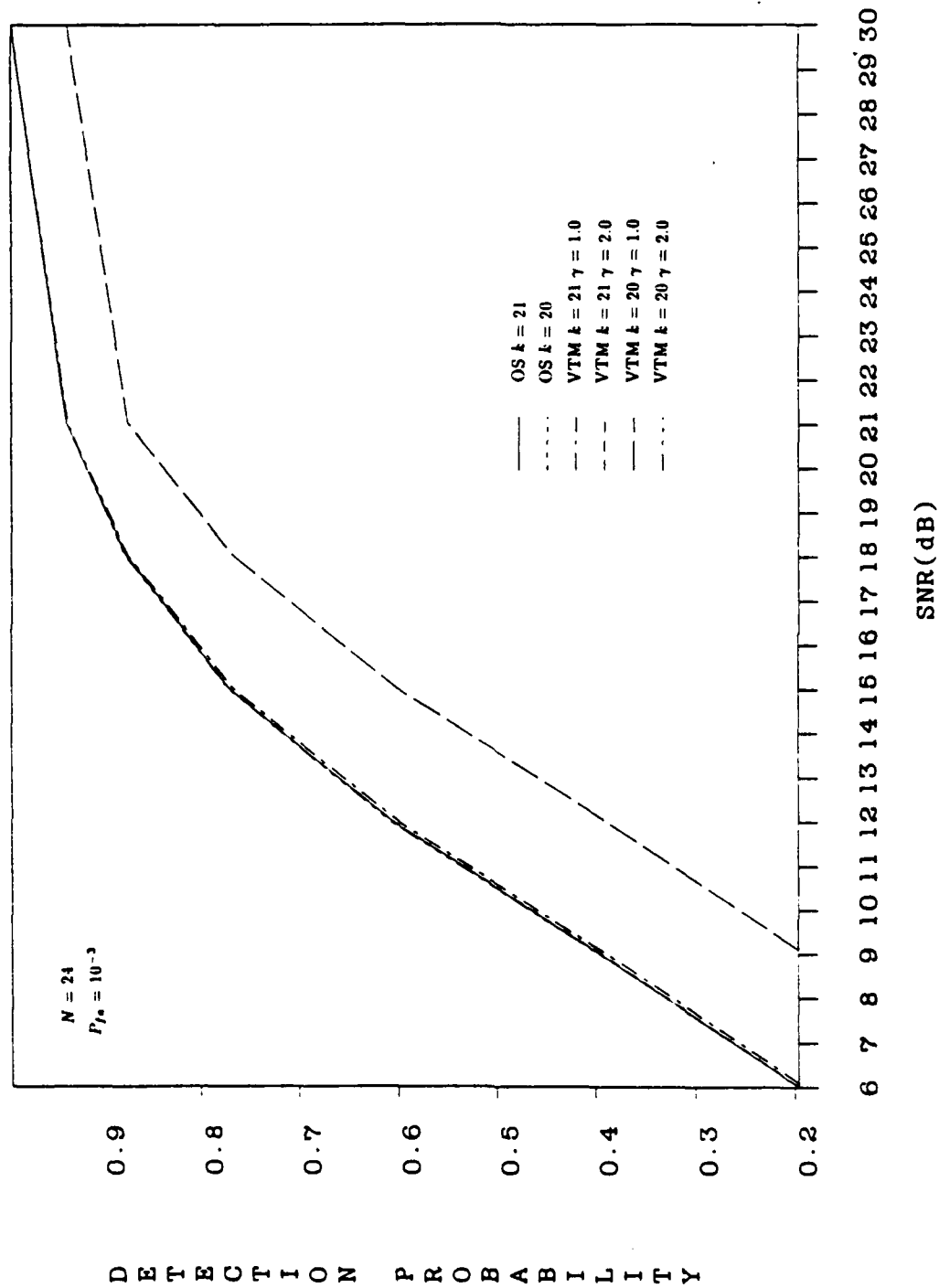


Figure 9 : Detection Performance of OS and VTM-CFAR processors in homogeneous background for selected parameters.

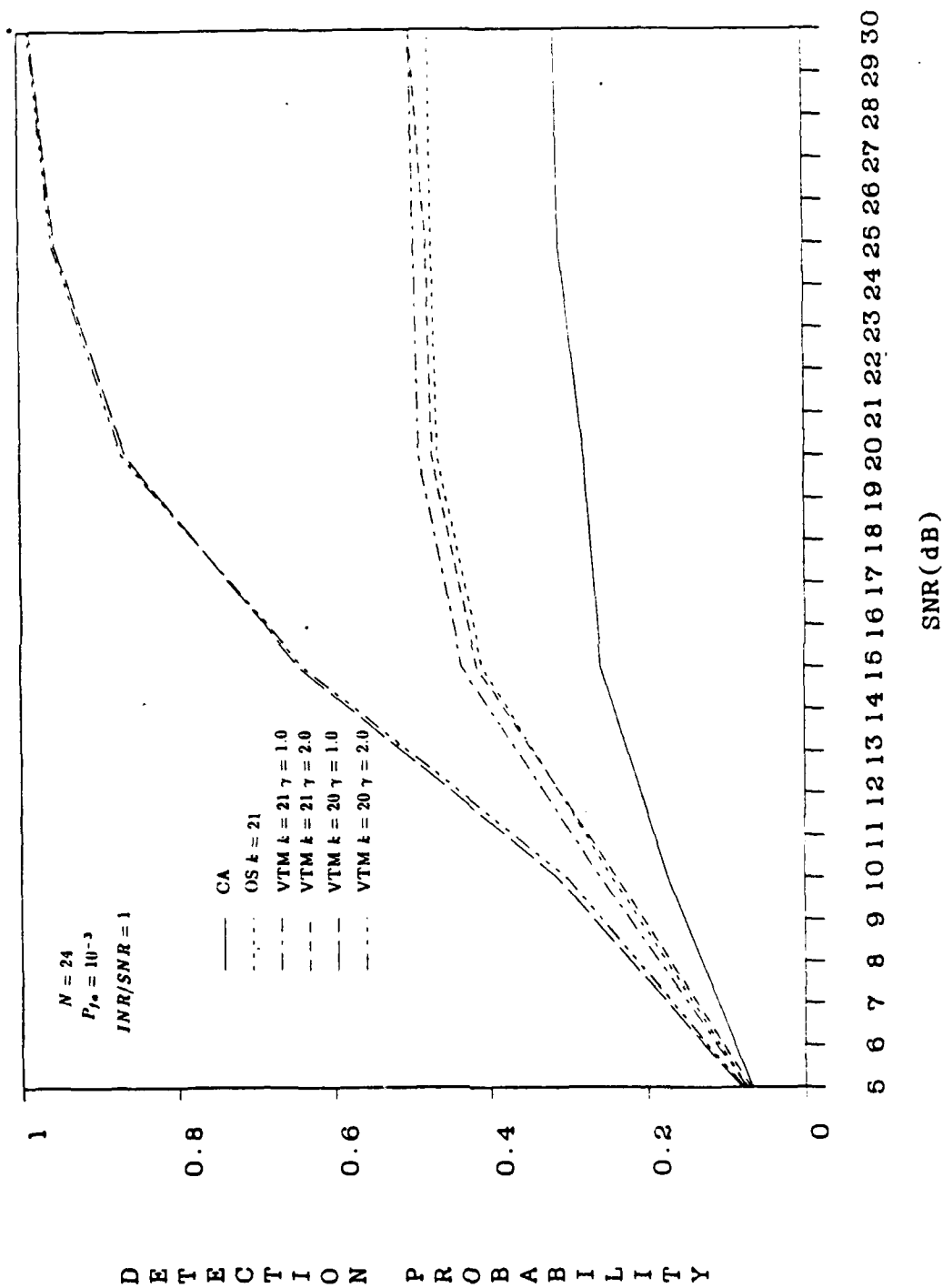


Figure 10 : Detection Performance of CA, OS, and VTM CFAR processors in presence of four interfering targets with selected parameters.

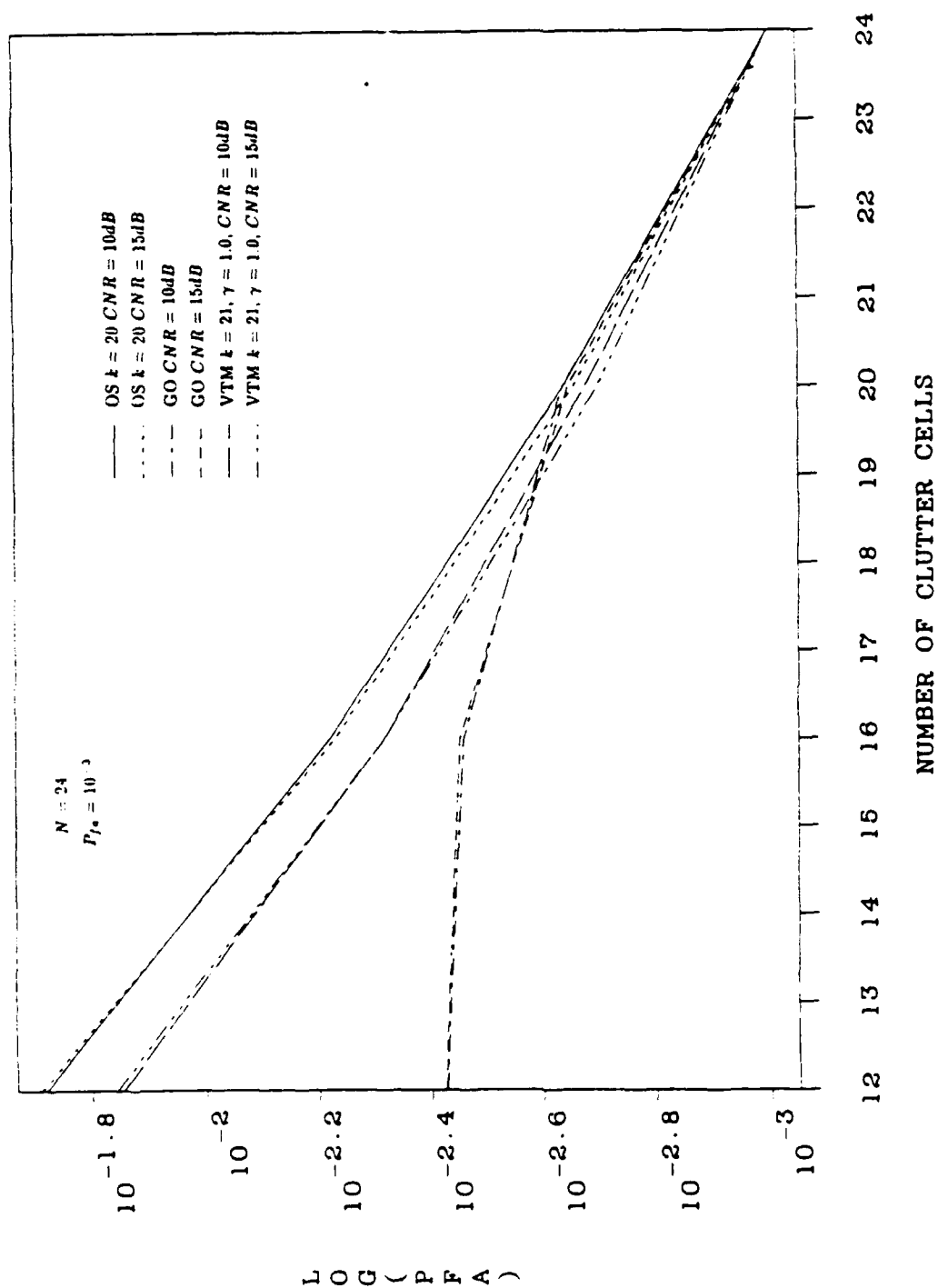


Figure 11 : False alarm rate performance of GO-, OS and VTM-CFAR Detectors in clutter power transition with selected parameters.

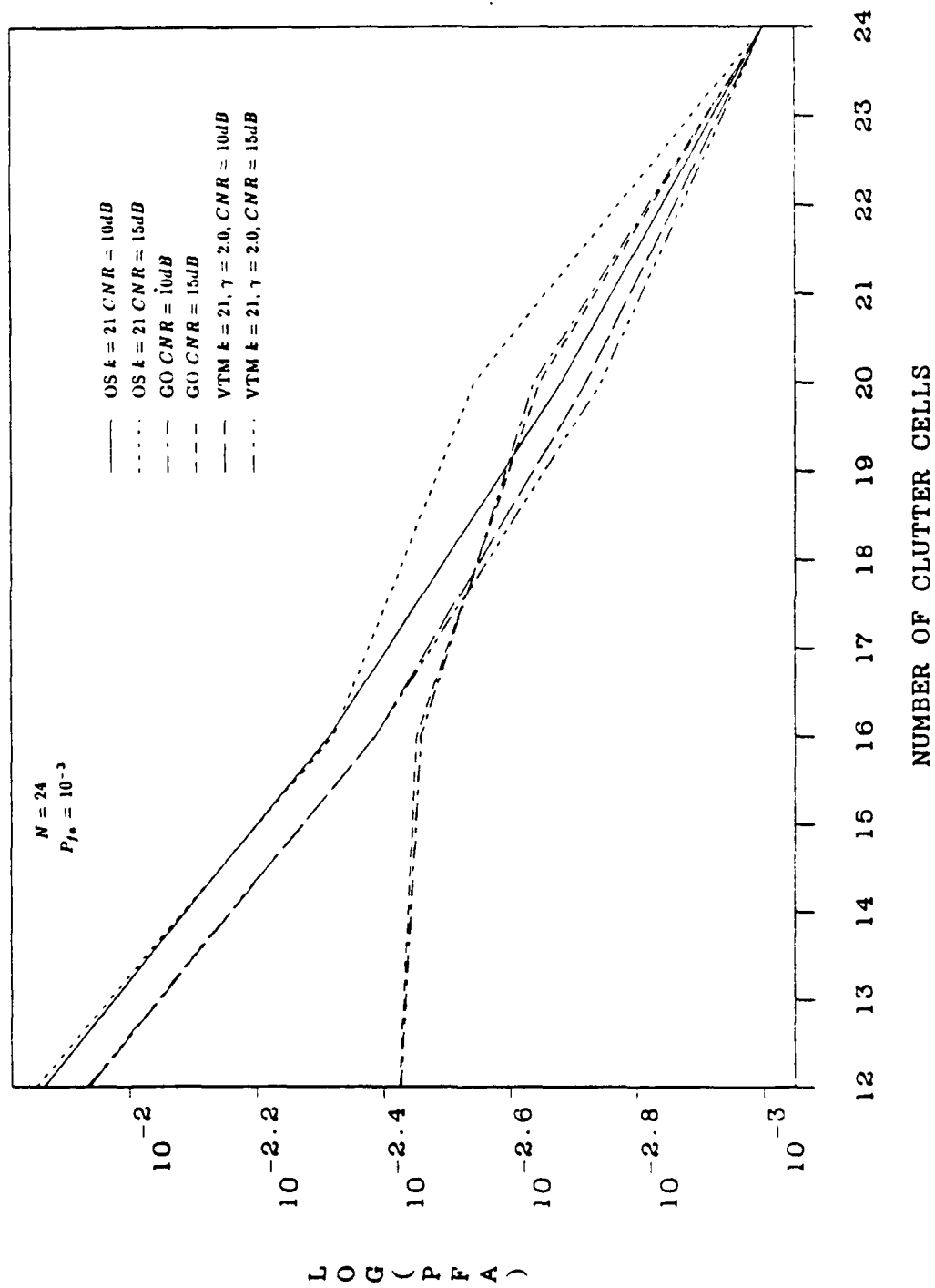


Figure 12 : False alarm rate performance of GO, OS and VTM-CFAR Detectors in clutter power transition with selected parameters.

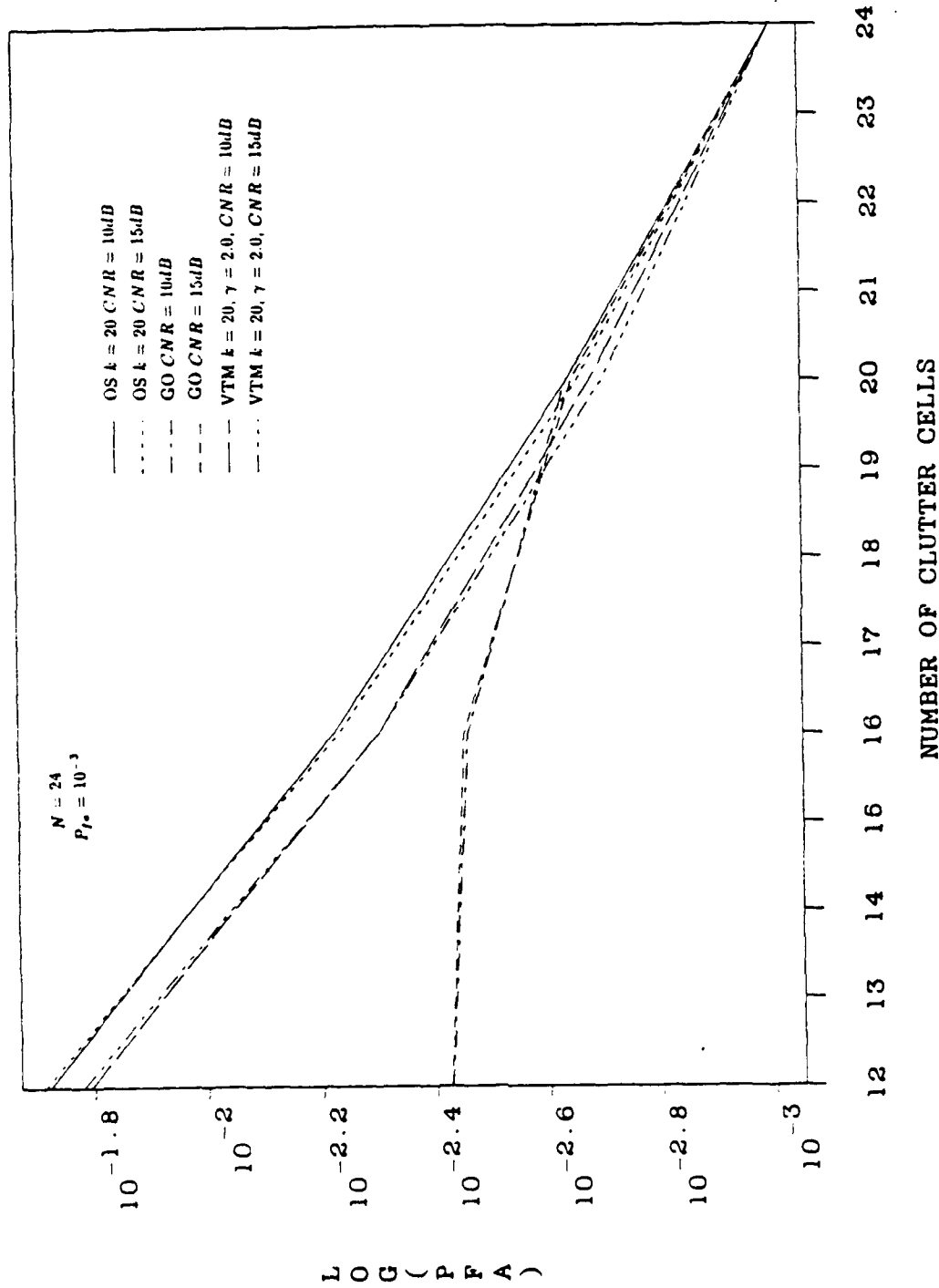


Figure 13 : False alarm rate performance of GO-, OS and VTM-CFAR Detectors in clutter power transition with selected parameters.



# *MISSION of Rome Air Development Center*

*RADC plans and executes research, development, test and selected acquisition programs in support of Command, Control, Communications and Intelligence (C<sup>3</sup>I) activities. Technical and engineering support within areas of competence is provided to ESD Program Offices (POs) and other ESD elements to perform effective acquisition of C<sup>3</sup>I systems. The areas of technical competence include communications, command and control, battle management information processing, surveillance sensors, intelligence data collection and handling, solid state sciences, electromagnetics, and propagation, and electronic reliability/maintainability and compatibility.*